

The use of a fully recyclable, biomass based thermoplastic as a wood coating

A thesis presented for the degree of
MSc Mechanical Engineering

Remco van der Maat

November 3, 2022

<i>FACULTY</i>	Engineering Technology
<i>CHAIR</i>	Production Technology

EXAMINATION COMMITTEE

<i>Chair</i>	prof.dr. J. Lange
<i>Supervisor</i>	dr.ir. M. van Drongelen
<i>External member</i>	dr. M.P. Ruiz Ramiro
<i>External member</i>	dr. J. Seyyed Monfared Zanjani

UNIVERSITY OF TWENTE.

Abstract

Polymers and plastics see a lot of use nowadays, but as useful as they are, it has also become clear that they can cause environmental issues. Thus a need for more sustainable polymers arises. These sustainable polymers should ideally provide similar functionality as common polymers, without the environmental impact. A biomass based thermoplastic has previously been developed, which provides a fully recyclable and thus sustainable alternative to common thermoplastics. The material can be produced from ligno-cellulosic biomass like pulp waste or wood and is produced through the liquefaction process. The end product is easily recycled through the same liquefaction process, forming a closed loop. While this is promising, research has to find useful applications for this material.

So far, the tensile strength is not very promising (0.4 MPa), but both short and continuous natural fibre reinforcement shows good improvement (2.3 MPa and 47.2 MPa respectively) and makes for a fully recyclable composite. While this may enable the use in structural applications, the thermoplastic itself is still quite brittle. The search for further applications thus continues.

The focus of this research is on wood coatings made from this 'woody thermoplastic' material, as it could provide a greener substitute to common synthetic paints and coatings. The use on natural substrates like wood again allows for fully recyclable end products. The thermal properties of the material are first investigated through rheology and DSC measurements. The melt behaviour is found comparable to other common thermoplastics as shear thinning is observed and the melt viscosity is in a similar order of magnitude. The glass transition temperature is found to be 47°C.

A primitive paint is made by dissolving the polymer in acetone. The paint is then brushed on plywood to form coating samples for further testing. The adhesion of the coating is tested by a dolly pull-off, where an adhesion of 1.2 MPa is found. The result is limited by the cohesive strength of the material, indicating that the adhesion to the wood is stronger than the cohesive strength of the material. Hydrophobicity is measured through the contact angle of a water drop on the coating and is determined at 72°, which is acceptable for a polymer, albeit somewhat on the lower end compared to other polymers.

Unfortunately, the coating properties quickly deteriorate when exposed to the outdoors, as found in a natural weathering test. Photo-oxidation due to UV exposure is expected to be the main cause of degradation and is therefore briefly discussed as a topic for future work.

Hence, to be useful as a coating, the material would have to be improved in strength and a proper paint may need to be formulated to improve the coating durability and resistance against degradation.

Contents

Abstract

1	Introduction	1
2	Previous work and related literature	3
3	Test methods	6
3.1	Rheology measurements	6
3.2	Differential Scanning Calorimetry (DSC)	7
3.3	Solvent painting	7
3.4	Weathering	8
3.5	Adhesion testing	10
3.6	Surface roughness	10
3.7	Hydrophobicity	11
3.8	Water permeability	11
4	Results	12
4.1	Rheology	12
4.2	Differential Scanning Calorimetry (DSC)	12
4.3	Solvent painting	14
4.4	Natural Weathering	14
4.5	Artificial Weathering	15
4.6	Adhesion	16
4.7	Surface roughness	17
4.8	Hydrophobicity	20
5	Discussion	22
6	Conclusion and recommendations	24
A	Appendix	28
A.1	Rheology, amplitude sweep	28
A.2	Rheology, storage and loss modulus	28
A.3	Submersed samples	31
A.4	Roughness data	31
A.5	Contact Angle data	33

1 Introduction

Plastics and environment

Thermoplastics like polypropylene (PP) and polyethylene (PE) are common sight in various applications, from everyday products and packaging to construction. But rising climate concerns lead to an increasing need of finding more sustainable alternatives. In 2015 about 380 million tons of plastic was produced and in the same year, plastic waste is estimated to be about 302 million tons, of which 55% was discarded into landfills, 25% was incinerated, and 20% was recycled (Geyer et al. 2017). A big problem with plastic waste that is discarded is pollution. The polymers degrade due to UV light and slowly break down into smaller particles: microplastics. The extent of the pollution is dependent on the management of the waste. Although pollution can be contained, degradation can not be prevented indefinitely.

Despite its issues, plastics are also (relatively) cheap and lightweight and thus advantageous to use for packaging, clothing, electronics and other products. Additionally, Ritchie 2018 states that using plastic packaging in the food industry led to a lower net environmental impact, due to reduction of food waste and reducing the use of other resources in the production chain. Another example is the shopping bag, Bisinella et al. 2018 analysed the environmental impact of shopping bag materials. It is found that organic cotton bags need to be reused 149 times to have the same climate change impact compared to LDPE bags. Bags made from recycled polymers, bio-polymers, and paper only need to be reused a handful of times. When considering a broader environmental impact (including toxicity, resource and water use, and others), the organic cotton bag should be reused 20000 times to have the same impact as the LDPE bags. The other bag materials only need 40-80 reuses to have the same impact as LDPE. This shows that polymers have their place when considering the environmental impact, but alternative materials and recycling should be considered.

Recycling of ‘regular’ plastics is luckily available, but is also limited and (of course) can’t solve the entire problem of plastic use. Plastic recycling is either done thermo-mechanically by grinding the plastic to pieces and processing them to pellets, it can be done thermally by heating the material and breaking down the polymer chains, or chemically de-polymerising the material to form new chains afterwards. Often, recycling of plastics produces lower quality plastics, which do not directly replace virgin plastics made of fresh resources. Recycling of waste plastic is also not always financially advantageous, compared to energy recovery through incineration (Gradus et al. 2017).

Improvements are still being made though, as Tournier et al. 2020 shows an improved depolymerisation of PET using hydrolysis, with more than 90% monomer yield after 10 hours. A different way to recycle end of life plastics is to convert them into bio-fuel allowing recovery of energy from waste material. Padmanabhan et al. 2022 reports the production of a bio-diesel blend produced from HDPE (high density polyethylene) through pyrolysis. A fuel blend is made which results in higher thermal efficiency, lower fuel consumption and reduced emissions compared to regular diesel fuel.

Even when considering fibre composites, which are inherently tricky due to the mix of fibre and matrix, have recycling options. Mechanical, thermal, and chemical methods are available, which allow the re-manufacturing of products from the recycled material. The new product may however not have the same properties from before recycling. (Oliveux et al. 2015; Pimenta and Pinho 2011)

Zheng and Suh 2019 conclude that in order to reduce greenhouse gas emissions from the plastic industry, all four of the investigated approaches (bio-based plastics, renewable energy, recycling and demand management) need to be implemented.

It is clear that plastic use has its pros and cons and the environmental impact is complicated and highly depends on the considered aspects. Since a product life cycle involves many steps each with their own influence, solutions also need to come from multiple angles, at every stage of the material. The work presented here focuses on the improvement that may be made at the beginning and end of a plastic product. By using renewable source material and ensuring recycle-ability at the end, the loop closes and in turn reduces the waste of material. Bio-based polymers may play a role in this step towards more sustainable plastic products.

Bio-based plastics

Bio-based plastics can be produced from biomass like potatoes (starch), corn, and wood (both cellulose), which are all a renewable resource. Using waste material from other industries is also an attractive option for source material. It should be noted that bio-based plastics are not necessarily biodegradable (although they can be both), bio-based versions of PE and other plastics are available, but they are not necessarily biodegradable. They do lower the carbon footprint due to sourcing from renewable materials, but might still possess the risk of pollution through microplastics. Ideally, a plastic would thus be both bio-based as well as biodegradable, or at least bio-based and fully recyclable. Either would reduce plastic waste, or the impact of such waste.

This thesis further investigates a previously developed thermoplastic material produced from wood ('woody thermoplastic'). The material is produced from biomass and is fully recyclable and hence a promising step in the search for sustainable polymers.

Woody thermoplastic

The production of the thermoplastic can be done by liquefaction. Liquefaction is a relatively simple and cheap process when compared to other multi-step methods involving fractionation. In short, liquefaction is done by heating biomass (wood in this case) together with a solvent in an autoclave with temperatures reaching 300°C and pressures of 60 bar. This process breaks down the molecule chains in the biomass. Some reasons for the use of biomass based thermoplastics are:

- Biomass is often 'waste' material from other industries, making it cheap and readily available as source material.
- When combined with natural materials, like natural fibres or wood, the biomass based thermoplastic ensures that the final product is fully recyclable through a circular process.
- It is not reliant on oil as a resource.

Thus in theory, the woody thermoplastic may provide a cheap and simple alternative to common thermoplastics. Research needs to find ways to put the theory into applications.

Objectives

Since the material is not developed for a particular purpose, the material needs to be further investigated to find out what it is useful for. As discussed later (section 2), previous work showed poor performance as bulk polymer, although fibre reinforced samples are more promising. Interest is therefore steered towards a different application: coatings. The interest in particular is to find out if the material is useful as a coating on wood substrates. Can it, for example, provide protection of the substrate like conventional paints and lacquers?

The main questions to answer are then:

- What makes a good coating material?
- Is the woody thermoplastic a suitable coating material?
- What production method is suitable to produce 'woody' thermoplastic coatings. Thus taking into account process-ability, substrate preparation, and possible recycle options, while avoiding non-sustainable components.

This thesis will attempt to answer these questions or at least provide enough insight for future work. The previous work done with the woody thermoplastic is discussed first, after which an overview of literature related to coatings is presented in section 2.

The properties of the woody thermoplastic are then further investigated and a basic coating is made and tested through a few experiments as described in section 3.

2 Previous work and related literature

The first section in the literature study will provide some more background information on the woody thermoplastic. This is done by consolidating some previous work done by J. Mijnders, B. Nogova, P. Ruiz, and others. Further sections will delve into thermoplastic coatings, thermoplastic bonding of wood, and wood coatings in general.

Biomass based ‘woody’ thermoplastic

Mijnders 2018 produced the bio based thermoplastic material from liquefaction of pine wood. Guaiacol is used as a solvent in the liquefaction process. In total, 6 consecutive process runs are done in order to increase the final molecular weight. Distillation of the resulting oil at vacuum and then at atmospheric pressure removed water and the guaiacol, and resulted in a thermoplastic with average molecular weight of 2500 Da. The melt trajectory was determined to be between 120°C to 150°C and a glass transition around 60 to 65 °C. Tensile tests show that the bulk material has a tensile strength of 0.4 MPa, hence fibre reinforced samples were produced afterwards. Using 20 wt.% continuous flax fibres achieved a 47.2 MPa tensile strength in the fibre direction, but the matrix material remains brittle. The zero shear viscosity is measured from 120°C to 170°C and decreases from 30000 Pa·s to just under 100 Pa·s.

Nogova 2019 attempted to reduce the brittleness of the material with two methods: by adding flexible side chains through transesterification, and by mixing in high-amylose cornstarch. The transesterification between guaiacol and methyl octanoate did not occur, so it was not further investigated. Adding in 40% wt. cornstarch, the material has a tensile strength of 2 MPa (compared to 0.4 MPa without starch), but is still as brittle. The starch did reduce the strong smell of the material, but also made it more susceptible to water, which limits the material’s applications.

Ruiz et al. 2019 produced the woody thermoplastic with a molecular weight of $M_w = 6000$ Da, with a density of 1.43 g/cm³, again through liquefaction of pine wood. Reinforcement of the thermoplastic with 10 wt% short bagasse fibres showed an increase in tensile strength from 0.4 MPa to 2.3 MPa. The recycle-ability of the continuous flax fibre reinforced material (see above Mijnders 2018), was tested by using the material as input for the liquefaction process, the produced oil has a similar molecular weight as the other product. Additionally, eucalyptus, beech, bagasse, hemp, and oak bark were tested as biomass, which all resulted in an oil product with similar molecular weight as the pine wood oil. Thus, all these products could be used to produce woody thermoplastic.

Wood coatings

The EN-927 standard is one of the standards that hold a series of tests for the assessment of (wood) coatings and can therefore be used to determine important properties and what tests to perform. The standard includes tests for: natural weathering, artificial weathering, adhesion, water permeability, impact, and other properties. For visual appeal the coating colour and gloss may also be of interest. As discussed later, ISO 16053 is used as a loose guide for a natural weathering test.

Norvydas and Minelga 2006 coated both sides of particleboard with various layers: a paper-based film, compensatory paper, laminated plastics, 1 to 8 layers of 0.6 mm mahogany veneer, and acrylic paint. For every coating, the bending strength f_m and the elastic modulus E was measured using a 3 point bend test. The acrylic paint did not increase the strength and modulus, but all other coatings did. The compensatory paper showed the smallest increase: from $E = 2001$ MPa to 2023 MPa (+1%) and from $f_m = 18.5$ MPa to 20.3 MPa (+10%). Five layers of veneer resulted in the largest increase: from $E = 2001$ MPa to 3528 MPa (+76%) and from $f_m = 18.5$ MPa to 52.2 MPa (+182%). Interestingly, 6, 7 and 8 layers each had decreased strength compared to 5 layers: 8 layers of veneer has $E = 3146$ MPa and $f_m = 47.8$ MPa, indicating an optimum strength at 5 layers.

When considering the thickness of the veneer layers, the bending strength increases from 0 mm to 3 mm layer thickness (0 to 5 veneers). From 3 mm to 4.8 mm (5 to 8 veneers), the bending strength decreases again.

Hazir and Koc 2019 investigated and compared properties of water based paint, solvent based paint, and powder coated MDF. The coatings were assessed on adhesion strength, coating hardness, layer thickness and rapid deformation tests. The MDF samples of 10x10x1.8 cm are all sanded on a belt sander with

150 grit sandpaper and are conditioned at 20°C and 65% relative humidity until the moisture content is 10%. A primer was applied on the substrates before the coating was applied. The mean results are consolidated in Table 1.

Table 1: Overview of results from Hazir and Koc 2019, mean values of multiple measurements. Rapid deformation test excluded.

Coating	Adhesion Strength [MPa]	Hardness [s]	Thickness [μm]
Water based	3.1757	288.67	163.8
Solvent based	2.1960	231.40	166.8
Powder coat	2.7173	327.23	187.7

The hardness test is performed with a König pendulum, measuring the time needed to dampen the pendulum oscillation (according to EN ISO 1522-2016). A shorter time indicates a lower hardness. The rapid deformation test results are excluded, since a score out of 5 was given based on visual damage. Hence, no quantity is measured, although the results indicated the powder coating deformed more than the other two coatings.

Thermoplastic coatings

Järvelä et al. 1999 showed that using extrusion is a viable method for coating plywood boards with polypropylene. Evaporation of moisture in the wood (due to the heat of the melt) caused bubbling in the coating, which was remedied by constraining the coating with light pressure. This pressure contained the vapour until the coating cooled enough to where it was strong enough to contain the vapour by itself. A heater is also placed before the extrusion die to assist in drying the substrate. A peel test resulted in a peel strength of 1.2 N/mm, while a button-pull tests showed that the adhesion between coating and substrate is 1.9 N/mm² (1.9 MPa).

Kuusipalo 2001 used a similar extrusion technique, but with polyethylene and 3 other adhesion polymers. IR heaters were placed at the start of the production line, to initiate the drying of the substrate. Additionally, a flame was placed just before the extrusion die to further heat and dry the substrate. Plywood with birch and pine top veneers were used as substrate, but no clear difference was found between the two. As in Järvelä et al. 1999, bubbling of the coating is again encountered. A melt temperature of 240°C showed less bubbling compared to a melt temperature of 315°C. Except the combination of a PVDC primed substrate with a CXA adhesion polymer, which also showed bubbling at lower temperatures. This combination did, however, produce the best bonding in areas without severe bubbling. Using an acrylate primer improved the adhesion without introducing additional bubbling (w.r.t. no primer use).

Thermoplastic bonding of plywood

Considering a possible application of the woody thermoplastic as a binder of plywood is interesting due to the full recycle-ability of the final product. Especially when compared to the phenol-formaldehyde based glues traditionally used in plywood production. More recent developments are towards using polymer melts as a binder.

Kajaks et al. 2009 investigated lap joints of two birch veneers with polyolefins as glue with the goal to find the optimum process parameters for the hot press process, in order to attain the highest shear strength. Shear strength values of up to 8-10 MPa are found by using polypropylene, which is stronger than conventional plywood (3.66 MPa). Increasing temperature, pressure and/or mass flow index (MFI) all resulted in reaching maximum shear stress quicker (within 1-2 minutes). Longer processing times did not improve the shear stress. The optimum parameters are determined at: 180°C, 1 to 3 minutes at 7 to 10 MPa pressure. However, at $T > 180^\circ\text{C}$ and $P > 10$ MPa the wood substrate may be compromised due to deformation or thermal degradation. Hence, these parameters must not be exceeded in the production process.

Concluding

So far, the previous work on the material is discussed, showing improvements in strength by fibre reinforcement. In search for a useful application of the material, the coating of wood is now of interest.

Test standards for (wood) coatings are used to determine important properties for testing the coating performance, like adhesion and weathering. From Hazir and Koc 2019 it can be expected that the adhesion is between 2-3 MPa.

From Järvelä et al. 1999; Kuusipalo 2001 it is clear that (with the right parameters), wood panels can be coated with thermoplastics by using extrusion. The adhesion of the resulting coating is 1.9 MPa.

As an alternative application of the woody thermoplastic, bonding of wood veneer could be considered for the production of plywood.

3 Test methods

A multitude of tests and measurements are done to better understand the material behaviour as well as its suitability as a coating. To start, the thermal properties of the material are investigated through rheology and DSC (Differential Scanning Calorimetry).

Afterwards, an approach to producing a coating is discussed. A simple paint is made by dissolving the polymer in acetone.

With a production method available, the properties of the coating can be assessed. The adhesion to wood is determined in both a qualitative (by tape-pull) and quantitative (by dolly-pull) way. The roughness of the surface is measured through confocal microscopy. The hydrophobicity of the coating is assessed by measuring the contact angle of a sessile drop. In addition, the water permeability of the coating is tested by submerging samples in water. Finally, a natural weathering test is done by placing samples outdoors. The adhesion, roughness and contact angle are assessed to track the properties throughout the weathering experiment. To further dissect the weathering, artificial exposure to UV is also done, again assessing adhesion, roughness, and hydrophobicity. For comparison, a commercial paint is tested alongside the woody thermoplastic.

3.1 Rheology measurements

Rheology measurements are done on the woody thermoplastic, since not much is known about its behaviour so far. Only the zero shear viscosity for various temperatures were measured previously (Mijnders 2018). Additional measurements provide more insight in the process-ability and overall flow behaviour.

The viscosity as a function of shear rate is measured to describe the expected non-Newtonian behaviour of the melt and form a flow curve. This is done with an Anton Paar MCR501 rheometer by rotational measurements where a disc of material is placed between two flat plates (plate-plate geometry). The rotational measurements are done at temperatures from 100°C to 160°C, with 10°C steps and shear rates between 0.1 s⁻¹ and 1000 s⁻¹.

Additionally, the visco-elasticity is determined by oscillating measurements, again with plate-plate geometry. An amplitude sweep is done to find the limit of the linear visco-elastic range. Then, a frequency sweep is done to find the loss and storage modulus, giving insight in the viscous and elastic components of the melt.

From the resulting amplitude sweep (see Appendix A.1, Figure 25), the maximum amplitude in the linear range is determined to be 1% strain. To be safe, initial measurements were done at 0.1%, but were found unusable at higher temperatures, thus 1% was eventually used for the frequency sweep. The frequency sweeps are done from 0.5 rad/s to 500 rad/s, again at temperatures from 100 to 160°C.

For the rheology measurements, disc shaped samples are prepared in a hot press (Fontijne 200) at 80°C with 15 kN of force for 10 minutes. After 10 minutes at 80°C, the samples are actively cooled inside the closed press to 30°C, after which they are taken out of the press and removed from the mould.

To prevent sticking, the plates on either side of the mould, are covered in aluminium foil. The foil and the mould itself are then treated with 227-CEE mould release agent. The mould consists of 25 mm holes cut in 1 mm thick steel plates (see Figure 1), such that the resulting samples fit neatly in the rheometer. The density of the material is previously determined to be 1.43 g/cm³ (Ruiz et al. 2019), thus in theory, the amount of material needed per sample is:

$$m_{sample} = \rho \pi \left(\frac{D}{2} \right)^2 t = 1.43 \cdot \pi \cdot 1.25^2 \cdot 0.1 = 0.702 \text{ g}$$

In practice, using about 0.65 grams of material yielded samples with less material spilling out the mould compared to 0.70 grams. Using 0.60 grams resulted in still usable samples, but these samples are not full discs as there are small gaps at the edges.

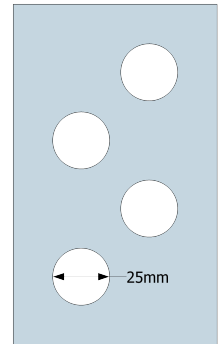


Figure 1: Drawing of the mould used to create rheology samples.

3.2 Differential Scanning Calorimetry (DSC)

In addition to the DSC measurement already done by Mijnders 2018, another DSC measurement is performed. Partially due to the ageing effect seen in the previous result (shown and discussed later in Figure 9), and partially to cover a larger temperature range. A small sample of the material is put in a TA DSC 250 and first cooled to -60°C where the measurement starts. The materials is then heated to 180°C , cooled once more to -60°C and again heated to 180°C . This ensures that any ageing effect is seen on the first heating cycle and not the second, while the glass transition temperature is then determined by the second heating cycle.

Naturally weathered material (explained later in 3.4) is also used for DSC measurements to investigate the influence of weathering on the glass transition.

The normalised heat flow to the sample is measured and plotted as a function of temperature. A change of slope in the curve then shows the phase transition(s) in the material.

3.3 Solvent painting

Regardless of the ideal coating method, it first needs to be known if the material is suitable as a coating. A simple way of applying the coating is with a solvent based paint. It is known that the material dissolves in acetone, which comes with the advantage that acetone evaporates quickly. Thus a quick drying paint can easily be made. The ratio of material to acetone is investigated.

However, acetone does not seem to fit in the sustainable approach of the woody thermoplastic, so ideally a different sustainable solvent would be used in the future, or a production method without any solvent is required. This is further discussed in section 6.

Substrate preparation is expected to be important to the adhesion, due to mechanical bonding at the interface. Initially a 14 mm thick plywood is used for the samples described here. The top veneer was found to thin, however, so a different 10 mm thick plywood was sourced for all other tests. Plywood (14 mm) samples of 10x10 cm are prepared in 4 different ways: no sanding, coarse, coarse and medium, and coarse to fine sanding. The grits used are: 80, 180 and 240. For each method, 3 samples are used as compiled in the following Table 2.

Table 2: Overview of samples and their preparation method.

Prep	Sample no.
No sanding	1-3
80 grit	4-6
80 + 180 grit	7-9
80 + 180 + 240 grit	10-12

Each sample is cleaned with alcohol, after which a 5x5 cm area is marked with painters tape, such that each sample has an equally large area coated. This also leaves holding space for potential testing. In order to keep track of the amount of thermoplastic that is deposited, each sample is weighed after sanding, and later after the paint has dried and the tape is removed. The difference is then the total material deposited.

For samples 1-3, 4.95 g of material is used in about 35 mL of acetone thus a ratio of 1g:7.1 mL, but not everything dissolved. The pieces of material were too big to easily dissolve. The material is thus crushed to smaller pieces, if necessary. For samples 4-12, the paint is prepared by dissolving 2.04 grams of woody thermoplastic in 11 mL of acetone, about 1g:5.4mL. The material is powdered and hence fully dissolves¹. The paint is applied with a brush and multiple layers are applied until there is good coverage (no substrate visible). The low viscosity of acetone makes it difficult to paint but does allow the paint to self level, resulting in a fairly even coating. The samples are left to dry for multiple days.

After drying, the film thickness is measured using a micrometer, by measuring the thickness of uncoated locations and of coated locations. Measurements are taken at multiple locations on the sample and averaged. This method is not the best approach and hence did not give adequate results. The film

¹Only based on visual appearance, small particles may be suspended but not dissolved.

thickness can also be approximated by the measured weight, density and area: $t = \frac{m_{paint}}{\rho A}$, where the area is known to be 5x5 cm. This does assume a fully solid layer without cavities. However, the weight measurements were not reliable and could not be used, thus a different approach is needed.

Since the film thickness is not determined, a new sample is painted. This time, the thickness is measured before and after coating, on the same locations. A stick of solid wood is sanded and 5 sections are marked and labelled A through E. Section A only gets one coat of paint, section B two coats, and so on, such that section E has 5 coats of paint. The sample is shown in Figure 2. The first two coats are done with

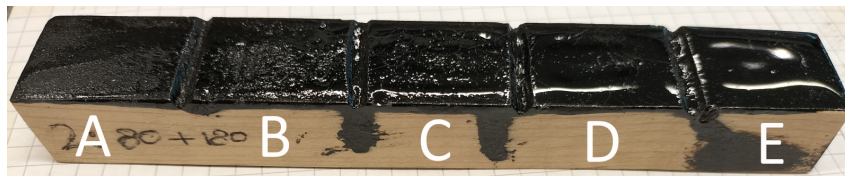


Figure 2: Image of the sample with 5 sections, each a different layer thickness. From left to right sections A through E with 1 to 5 layers of paint respectively.

2.01 g material in 11 mL acetone, a 1g:5.5 mL ratio. More paint had to be made afterwards, this time using 6.10 g in 12 mL, thus increasing the ratio to 1g:2.0 mL. This paint is used for the third, fourth and fifth coat and may lead to thicker coats for those sections. Despite the increased ratio, the paint itself is still quite thin (low viscosity) and thus still messy to apply.

The thickness of the bare wood is measured at 9 points per section, which are marked on the bottom. After painting the thickness is again measured on these 9 locations, the difference is then the coating thickness.

Coating tests

For further testing, a commercial paint is used alongside the woody thermoplastic (WTP) material. As long as the time allows, the tests in the following sections are performed on both coatings, such that a comparison can be made. The commercial paint used is *Rambo Pantserbeits*² (hereafter referred to as ‘Rambo’) in a deep black colour, similar to the colour of the WTP. The paint is technically designated as a stain, but it does form an opaque, covering, coating on the wood, again similar to the solvent paint of the WTP.

3.4 Weathering

The tests laid out in the next sections 3.5-3.8 are used to assess the weathering of the coating. The tests are performed before and after weathering of coated samples. Before describing those test, the weathering itself is first discussed.

Weathering will give insight in the degradation or any alteration of the coating by exposure to UV light, moisture, and temperature changes. Almost all polymers are susceptible to degradation outdoors, so it is expected that the woody thermoplastic is no exception. The discussion in section 5 will also attempt to explain the effect of the weathering on the WTP polymer specifically.

Weathering can be done by two different approaches: natural and artificial weathering. For natural weathering, the ISO 16053:2018 standard is used as inspiration for the procedure. Fully adhering to the standard was deemed unnecessary, since it is currently not the goal to produce a coating that conforms to a certain standard. The weathering test is done by leaving samples outside for as long as this project allows, which is 11 weeks. This means that the results are an intermediate result, since a full weathering test should last 12 months per the standard. Plywood pieces of 10x10 cm and 10 mm thick are used as substrate. The pieces are sanded with 180 grit sandpaper and then cleaned with alcohol. The samples receive two coats on one face only, with about 24 hour drying time in between applications. At least another 24 hours is between the final coat and the start of the weathering test.

The samples are spaced out on an angled rack such that they are at 45° from horizontal. The rack is placed on a tiled, south facing balcony. See Figure 3.

² *Rambo* is part of *PPG Coatings Nederland B.V.*, Uithoorn, The Netherlands. Product purchased in May 2022

The natural weathering is done on WTP coated and ‘Rambo’ paint coated samples. Three sets of two samples per coating are weathered, thus 12 in total. This allows two samples of each coating to be assessed after 1 week, 4 weeks, and 11 weeks.

Artificial weathering allows separation of the influences, such that only the UV, or temperature, or moisture influence can be investigated.

For UV exposure, a CAMAG UV lamp is placed in a closed box together with 6 samples of each WTP coated, and ‘Rambo’ paint coated plywood. Six samples again allow for two samples for three different assessment times. The wavelength of the light is 366 nm and has an intensity of 14 W/m^2 at a distance of 17 cm, per the manual (CAMAG 2016) of a newer model. The actual distance between the lamp and the samples is 10 cm, thus increasing the irradiance.

To get an equivalent exposure similar to the natural weathering, the artificial exposure time is calculated.

Assuming 12 hours per day of sunlight with an intensity of 0.5 W/m^2 at 366 nm (National Renewable Energy Laboratory n.d.) means that the lamp is 28x more intense. To get 7 days (84 hours sunlight) natural exposure equivalent, the lamp should be on for $84/28 = 3$ hours.

Since the lamp has a 10 minute shut-off timer that can’t be overridden, the exposure is limited to these 3 hours (7 days natural equivalent). This also allows comparison to the 7 day natural exposure samples.

Since there are samples available for 3 separate time steps, intermediate exposures of 26 minutes and 77 minutes (12h and 36h natural equivalent) are done. Table 3 shows a quick overview of the exposure times.

After the exposure, the adhesion, contact angle and roughness are measured and compared to the reference measurements taken before weathering.

An overview of the weathering tests and their duration is shown in Table 4.



Figure 3: Picture of the natural weathering setup. The samples are stapled to the chicken wire at the back. The rack is angled 45° and faces south.

Table 3: Equivalent exposure times for artificial and natural UV exposure. Assuming 12 hour sunlight per day with an intensity of 0.5 W/m^2 at 366 nm and using a UV lamp with 14 W/m^2 .

Artificial time	26 min.	77 min.	180 min.
Natural time	12 h.	36 h.	84 h.

Table 4: Overview of the test duration performed on both WTP coated and ‘Rambo’ coated wood samples. The water submersion test also uses bare wood samples.

Test	Assessment time [days]		
	t_1	t_2	t_3
Natural Weathering	7	28	77
UV exposure ¹	1	3	7
Water submersion	4	8	18

¹ Natural equivalent time is listed, see Table 3 for actual exposure time.

3.5 Adhesion testing

Adhesion of the coating to the substrate is an important property, since bad adhesion would mean that the material is not well suited as a coating.

Qualitatively, the adhesion is assessed with a tape peel test. The test is performed on 4 plywood samples of which the surface is prepared differently (see also Table 2): one not sanded, one sanded with 80 grit, one sanded with 80+180 grit and one sanded with 80+180+240 grit. The coating is applied after wiping the surface clean with alcohol. While the exact coating thickness is unknown, all 4 samples are painted at the same time and visually look the same, so it is assumed that the coating thickness is roughly equal. Two overlapping crosses are cut into the coating using a knife (see Figure 4), loose particles are removed of the surface and pressure sensitive tape is then applied. After one minute, the tape is quickly and smoothly pulled off at 180° (adhesive side thus facing upwards). The coating is visually assessed for damage. The pulled off tape is stuck to a piece of paper and is also assessed. As seen later in Figure 13.

To quantify the adhesion, dolly pull off tests are performed with a PosiTest AT-M manual adhesion tester. Aluminium dollies with 20 mm diameter are glued to the coating using two component epoxy (see Figure 5). The cylinder of the device is attached to the dolly, and the device is slowly primed to just under 0.7 MPa, per the manual. The pressure is then further increased at a rate of about 0.25 MPa/s until separation of the dolly. The maximum achieved pressure is displayed by the device. Six tests are performed per sample.

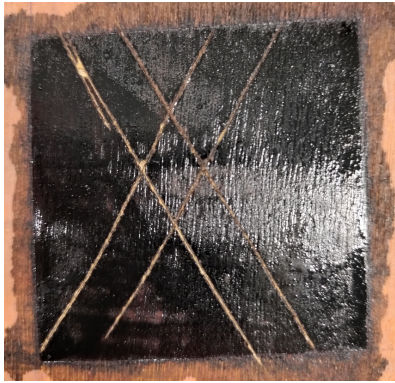


Figure 4: Coated plywood sample showing the cross-cuts for the tape pull-off test.



Figure 5: Image of the dolly glued to the coating.

3.6 Surface roughness

Measuring the surface roughness can provide interesting data on the coating and gives a better idea of what the surface looks like and how it behaves on a smaller scale.

The surface profile is measured using confocal microscopy. A Keyence VK9710 microscope is used with a 10x and 50x Nikon objective. At 10x magnification, an area of 5000x5000 μm is measured with a z-pitch of 2 μm . At 50x magnification, an area between 1000x1000 μm and 1500x1500 μm is measured with a z-pitch of 0.2 μm , depending on available measurement time.

Common parameters extracted from the height profile are the average roughness R_a and the root mean square (RMS) roughness R_q . The highest peak and lowest valley w.r.t. the mean, R_p and R_v , are also noted. These parameters provide single numbers to characterise the surface roughness and make comparisons but of course do not provide a full description of the surface. Additionally, a height distribution in the form of a probability density function (PDF) can be used to show more information about the surface. This is often accompanied by the skewness (S_k) and kurtosis (K_s) values, indicating the deviation from a Gaussian distribution.

The results will mainly focus on the single number parameters (R_a , R_q ,...) for simplicity.

Other information that could be gathered include the autocorrelation, power spectrum, RMS slopes, and RMS curvatures. These parameters will not be discussed, however.

Roughness data may also be used in determining contact behaviour between the coating and another

surface, but that is out of the scope of this study.

Measurements are done on woody thermoplastic coated plywood as well as a non-coated piece of plywood, to compare the coating to bare wood. The influence of coating thickness is also investigated by measuring samples 2A-E (Figure 2). It is expected that the initial thickness increase gives a smoother surface, since the thinnest coating looks rougher than the thicker coated sections.

As discussed in subsection 3.4, roughness measurements are also used to assess the impact of weathering on coated samples.

3.7 Hydrophobicity

A good indication of the hydrophobicity of the coating is the contact angle between the surface and a drop of liquid on top of the surface.

As an initial test, the contact angle is measured on a coated piece of plywood and a non-coated piece, to determine the difference that the coating makes. The sample from Figure 2 with different coating thicknesses is also used, to see if there is a relation between coating thickness and contact angle. It is expected that perhaps the thinnest coating has a reduced contact angle, because it visually looks rougher/less shiny than the other sections.

To measure the contact angle a drop of water is put on the coating, then the drop is photographed from the side such that the contact angle can be determined. A Nikon D3300 DSLR is used with a Nikon 18-55 mm lens attached via macro rings of 52 mm. The images are analyzed using ImageJ with the contact angle plugin (Brugnara 2006). The plugin requires manual point placement at the two ‘corners’ of the drop, and three points along the perimeter. A circular and elliptic fit are made on the drop, from which the contact angle with the baseline is determined. Figure 20 shows an image of the output of the plugin.

For each sample, 5 individual drops are photographed with exception of the bare wood sample. The bare wood adsorbs the water quite quickly, so a drop of water does not sit on the surface long enough. Thus for the bare wood, a single drop is photographed with 4 consecutive pictures over time.

For the weathering assessment, the same approach is used for the measurement of the contact angle.

3.8 Water permeability

To test how much water either permeates or is absorbed by the coating, samples are partially submersed in water for 18 days. Two uncoated samples, two WTP coated samples and two ‘Rambo’ paint samples are used. The samples are sticks of pine wood which are coated half of their length. A second copy of the samples is kept dry to keep track of any atmospheric changes in the lab. To determine the influence of the submersion, the weight, dimension (width and height) and visual appearance are recorded before submersion and then after 4, 8 and 18 days. This should give an overall idea of how much water has been absorbed and how much it affected the wood underneath.

A schematic of the setup is shown in Figure 6, the samples are held by a screw put into the uncoated end. The samples are suspended in a cup of water at the appropriate height by a piece of thread wrapped around the screw.

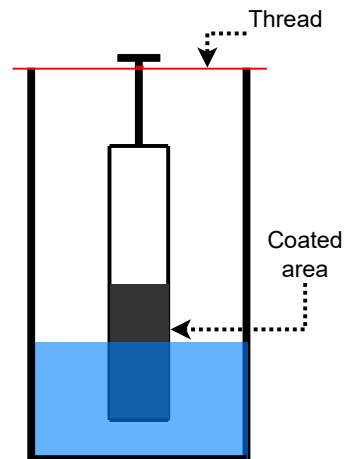


Figure 6: Schematic view of the water permeability test setup, showing a stick of wood which is half coated and suspended in water by a screw and some thread.

4 Results

4.1 Rheology

The viscosity of the material is measured through plate-plate rotational rheology. For the flow curve, shear rates from 10^{-3} s^{-1} to 10^3 s^{-1} are used, although values under 10^{-1} s^{-1} were omitted, since they contained too much error. At these shear rates, the shear stresses were likely too small for the rheometer to measure properly. The flow curve of viscosity η vs. shear rate γ is shown in Figure 7. As may be expected, it is seen that the viscosity reduces with increasing temperature. Shear thinning behaviour is also observed, as the viscosity drops with increasing shear rate. This data gives information for possible processing methods, which is discussed later on.

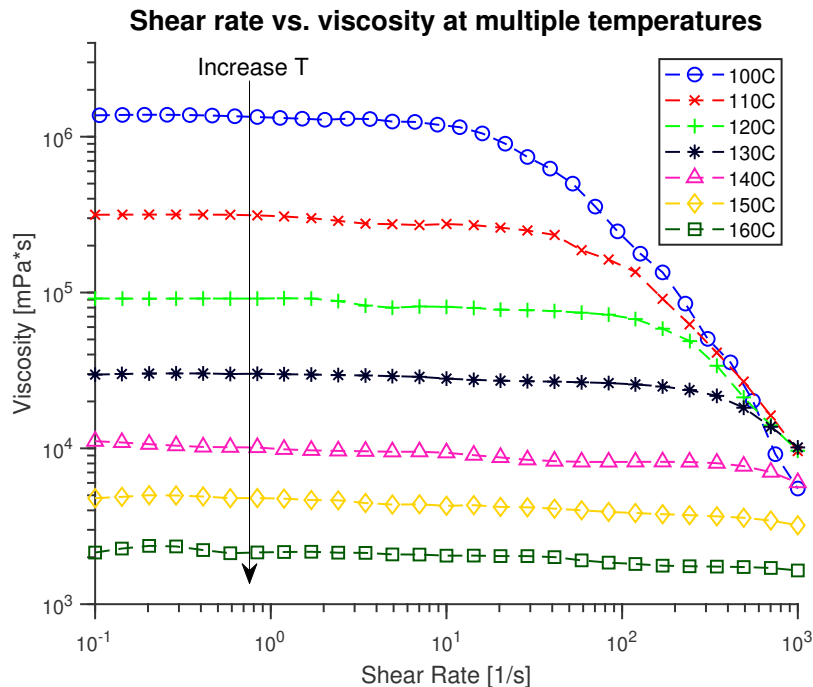


Figure 7: Flow curve of the ‘woody’ thermoplastic, showing viscosity as function of shear rate for temperatures of 100 to 160°C

Additionally, measurements regarding the storage and loss modulus are performed. These results are discussed in Appendix A.2, since they are not used further in this work.

4.2 Differential Scanning Calorimetry (DSC)

The result of the additional DSC measurement is shown side-by-side with the result of Mijnders 2018 in figures 8 and 9.

As indicated in Figure 8, the glass transition temperature is determined at $T_g = 47^\circ\text{C}$, about 15°C lower than what Mijnders 2018 found. The difference may be due to differences between material batches, since the molecular weight can differ per produced batch.

Also seen in Figure 8 is the ageing effect in the first heating curve. Due to ageing, the polymer chains initially require more effort to loosen when heated. This is reflected in the steep bump at 50°C , indicating a larger heat flow to the sample necessary to further increase the temperature. This bump is not present in the second heating cycle, since the polymer did not get the chance to age.

This ageing effect is also seen in the previous results of Mijnders 2018, albeit not so extreme as with the current results.

In Figure 10 the two DSC heating cycles of the weathered samples are shown together with the non weathered data. Note that the data is vertically adjusted, such that the curves initially overlap at $y = 0$.

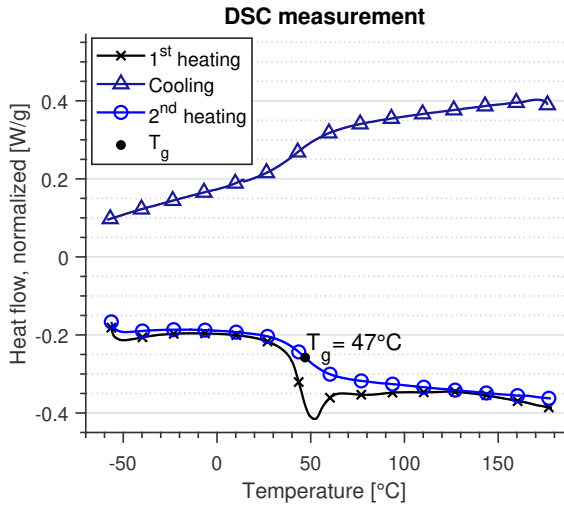


Figure 8: Current DSC measurement showing two heating and a cooling cycle. The first heating cycle shows a bump due to physical ageing, while the second heating step is used to determine the glass transition temperature of 47°C

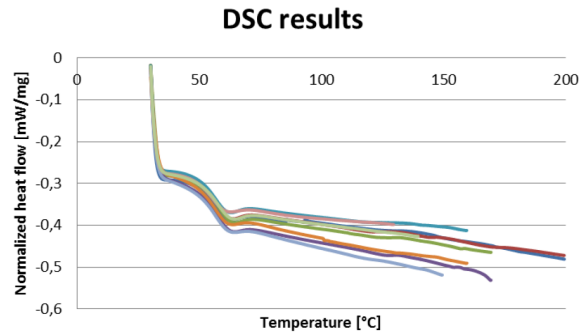


Figure 9: DSC results of Mijnders 2018 as taken from their report, showing multiple heating cycles from room temperature to various maximum temperatures. The glass transition temperature is determined at 60-65°C.

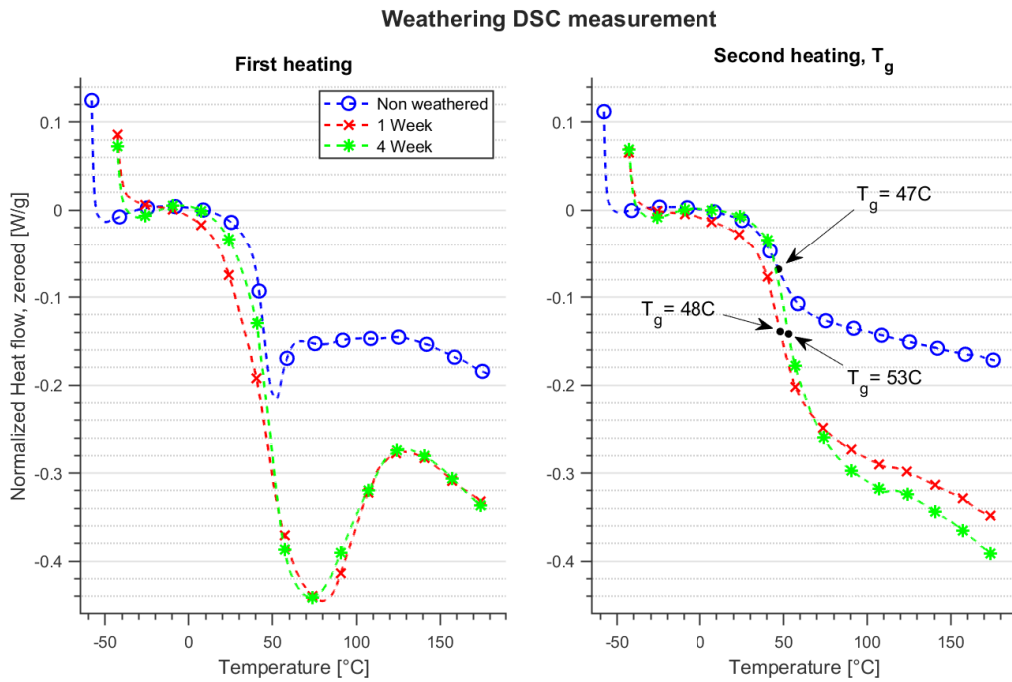


Figure 10: DSC measurement of weathered samples, compared to a non weathered sample. The data is vertically adjusted such that the curves initially overlap $y = 0$.

Left: plots of the first heating cycles, showing the effect of physical ageing around the glass transition temperature (wider 'bump' in the heating cycle).

Right: the second heating cycles are shown, the ageing effect is now not present allowing determination of the glass transition temperature.

On the left, the first heating is shown, again showing the bump of physical ageing. It is clear that the weathering affected the material, as the bump is more pronounced compared to the non weathered measurement. The curves of the two weathered samples overlap fairly well. The main difference is the

1 week weathered curve already decreases under 0°C, while the 4 week and non-weathered curves start to go down between 10°C and 20°C. On the right, the second heating cycle is shown. Now the physical ageing effect is not present and the glass transition temperature is determined. A slight increase in T_g is observed due to the weathering, increasing from 47°C, to 48°C and 53°C after 1 and 4 weeks weathering. It is also obvious again that the weathering affected the material, as more energy is required to heat the sample. It is suspected that the weathering affected the chemical structure of the material, this will be discussed further in section 5.

4.3 Solvent painting

The weights of the samples before and after painting are presented in Table 5, however, the weight is actually less with the coating applied. Perhaps the moisture content of the samples changed between application of the paint and the weighing. Although the samples were already in the room for a while before painting, the temperature and humidity may not be constant. Another possibility is that the acetone may have driven out some moisture and thus reducing the weight.

Table 5: Weights of paint samples, before and after applying the paint

Sample	1	2	3	4	5	6	7	8	9	10	11	12
Weight before [g]	84.69	82.61	82.02	78.49	78.46	79.06	74.42	77.92	74.52	78.50	74.14	79.74
Weight after [g]	84.17	82.22	81.47	77.89	77.93	78.41	73.96	77.53	74.00	77.84	73.54	79.04
Difference [g]	-0.52	-0.39	-0.55	-0.60	-0.53	-0.65	-0.46	-0.39	-0.52	-0.66	-0.60	-0.70

The average thickness per section are shown in Table 6. As seen, the first coat is rather thin, the consecutive coats are much thicker. The first coat is likely to partially fill gaps in the rougher surface of the wood, reducing its effective thickness. Consecutive coats can sit on top of the smooth previous coat and are thus thicker. Also shown in the table are the standard deviations of the nine measurements per section, showing that the thicker coatings also have larger deviations in them. Although section A with a single coat has the largest standard deviation with respect to the coating thickness. Coats 3 through 5 on sections C-E were done with a higher ratio paint, but there is no clear influence on the coating thickness.

Table 6: Average thickness from 9 measurements on the painted wood for 5 different sections (A-E) with 1 to 5 layers of paint.

Section	A	B	C	D	E
No. of coats	1	2	3	4	5
Avg. Thickness [μm]	9.9	50.4	70.0	134.9	173.9
Standard deviation σ	8.2	9.5	17.4	19.3	24.2

The used ratios of woody thermoplastic to acetone throughout the project ranged from 1g:1.16mL to 1g:6mL. All paint was manually measured and stirred.

At the lower end (1g:1.16mL) the material does not fully dissolve. A ratio around 1g:3mL seems better, although it is difficult to visually assess if all material has dissolved. Since large chunks of material need to be avoided and thus fine powder is used, it can be that the powder is simply suspended in the acetone, and not dissolved.

4.4 Natural Weathering

A visual inspection of the weathered samples is first presented in Figure 11 and Figure 12 for the WTP and ‘Rambo’ samples respectively. The images show the samples at 0, 7, 28, and 77 days of natural weathering. Degradation of the woody thermoplastic coating is already visible after 7 days of natural weathering. The 0 day (reference) sample does have small cracks, which form even when the samples are kept indoors. The coating also has some texture due to the blue workshop paper used to store the samples.

Within 7 days the coating starts to blister and form more cracks over the whole surface. Between 7 and

28 days the coating wears off and the wood substrate becomes visible. The grain of the wood now appears as long cracks in the coating. At the end of the test, after 77 days, the WTP coating almost entirely comes off the wood. The substrate is partially exposed and the coating has become powdery and is easily removed from the wood.

Compared to the 'Rambo' coating, which does not seem to degrade at all during the testing time. This is, of course, to be expected from a commercial product that is specially formulated to protect wood outdoors.



Figure 11: Cropped images of the WTP coated samples to visually compare natural weathering effects. Left to right: 0 (reference), 7, 28, and 77 days natural weathering.

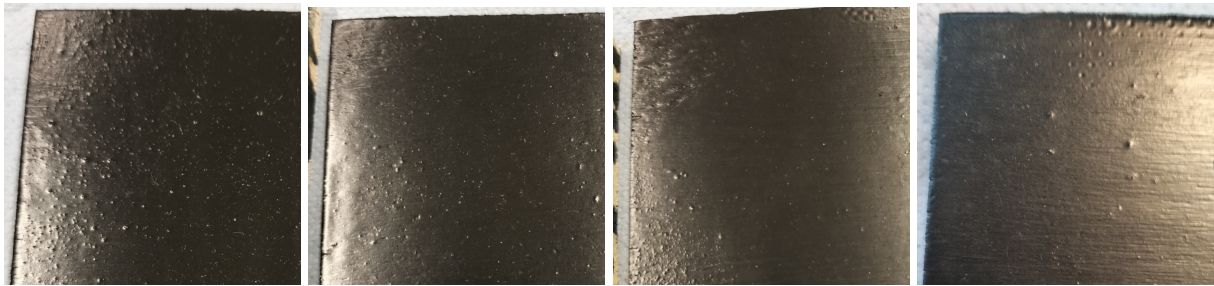


Figure 12: Cropped images of the 'Rambo' coated samples to visually compare natural weathering effects. Left to right: 0 (reference), 7, 28, and 77 days natural weathering.

The results of the adhesion, surface roughness, and hydrophobicity measurements on the weathered samples are included in the sections 4.6-4.8 of each measurement.

4.5 Artificial Weathering

Visually, the coatings did not change due to the UV exposure, thus no images are presented here. As with the natural weathering, the adhesion, surface roughness, and contact angle data is presented in their respective sections.

The submerged samples were assessed on weight and size, their weights are shown in Table 7. First note that the reference samples only varied in weight by 0.1 g at most, so any change larger than 0.1 g is due to the water submersion, not the room humidity. Both woody thermoplastic samples gained about 1.5 g after 18 days, indicating that some moisture has been absorbed. Most likely by the coating itself, as polymers tend to absorb some water. The colour of the surface also changed towards brown as shown in Appendix A.3 Figure 29

The 'Rambo' coating gained about 1 g over the 18 days.

The bare wood, being rather absorbent, ended up 5-6 g heavier than at the start. It also fluctuated a lot more, it gained about 7 g in the first 4 days, then lost about 3g, to then again gain 1-3 g. Considering water absorption, both coatings perform better than bare wood. The woody thermoplastic absorbed a bit more than the 'Rambo' coating. Since the woody thermoplastic is a polymer, absorbing moisture may affect some of its properties, but this was not investigated.

Table 7: Weight of the submersed samples over time. Two samples are used per coating, and bare wood samples are also used. The last three entries are reference samples which are not submersed.

Time [days]	0	4	8	18
	Weight [g]			
WTP 1	25.79	26.49	26.53	27.44
WTP 2	26.06	26.95	26.91	27.74
RM 1	25.23	25.58	25.60	26.22
RM 2	23.49	24.22	24.28	24.83
Bare 1	22.66	29.56	26.78	27.64
Bare 2	23.64	29.37	26.52	29.43
WTP ref.	19.86	19.86	19.73	19.80
RM ref.	30.16	30.15	30.01	30.04
Bare ref.	30.05	29.96	29.72	29.77

4.6 Adhesion

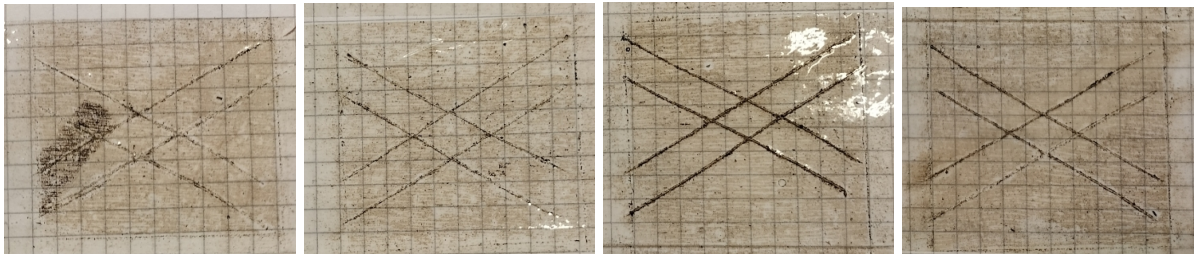


Figure 13: Image of the tape after the pull-off test, showing some material removed around the cut marks, as well as a slightly darkened square of removed material.

The tape peel test did not pull off the coating in a significant manner, as shown for the 4 samples in Figure 13. Some particles can be seen on the tape around the cut locations, and overall a thin layer is removed from the surface since the tape is somewhat discoloured. For all 4 samples the coating and tape looked very similar, thus no clear difference is found with respect to surface preparation. The darker cuts on the right two tape pieces are due to pressing the tape harder around the cuts. This was only done on the 3rd and 4th test, as with the second test some air was observed under the tape.

Overall, the coating adheres quite well to the wood substrate. With exception of the area just around the cut, where the coating is most likely damaged from the cutting, thus allowing some small pieces to be pulled off.

For the weathered samples, the dolly pull-off tests values are presented in Table 8. The woody thermoplastic coating initially fails around 1.19 MPa without any weathering. The failure is cohesive, as the coating adheres to both the wood and the dolly as shown in Figure 14. After 1 week of natural exposure, the adhesion is now 0.89 MPa with cohesive failure observed in the coating. After 4 weeks, the adhesion increases to 1.81 MPa. This increase is due to the degraded coating exposing more of the substrate, such that the dollies are partially glued to the wood underneath. Some splinters are also pulled out by the dollies.

For the ‘Rambo’ samples, an initial adhesion of 2.02 MPa is found, after 1 week this is 3.49 MPa and after 4 weeks this is 2.61 MPa. However, the failure is a mix between glue-coating and substrate failure as seen in Figure 15. Thus the found values depend more on the glue strength and the plywood (inter-ply) strength. The actual adhesion is thus difficult to determine, but most likely in the 3 - 3.5 MPa range.

For the UV exposed samples, the adhesion values are also shown in Table 8. The woody thermoplastic did not appear to be influenced by the particular UV wavelength, as the adhesion value do not change significantly. Mean values of 0.96 MPa, 0.96 MPa and 1.08 MPa for UV exposure times of 1 day, 3 days, and 7 days natural equivalent.

Table 8: Results for the dolly pull-off test, showing the maximum pressure (in MPa) reported by the measuring device. Results are averaged over 6 measurements and the standard deviation also reported. Failure mode is included between brackets: where (c) is cohesive failure of the coating, (g) glue failure, (s) is substrate failure, and (a) is adhesion failure of coating to substrate.

Coating	Sample: Ref.	Natural weathering			UV			
		t_1	t_2	t_3	t_1	t_2	t_3	
WTP	Mean pull-off force [MPa]	1.19(c)	0.89(c) ¹	1.81(cg) ¹	2.66(gs)	0.96(c)	0.96(c)	0.31(c)
	Std. deviation [MPa]	0.12	0.20	0.37	0.20	0.16	0.12	0.10
'Rambo'	Mean pull-off force [MPa]	2.02(cg)	3.49(cgs)	2.61(gs)	2.79(g)	2.53(ag)	2.95(acg)	3.46(cgs)
	Std. deviation [MPa]	1.17	0.18	0.28	0.40	0.12	0.34	0.18

¹ Only 5 usable measurements.

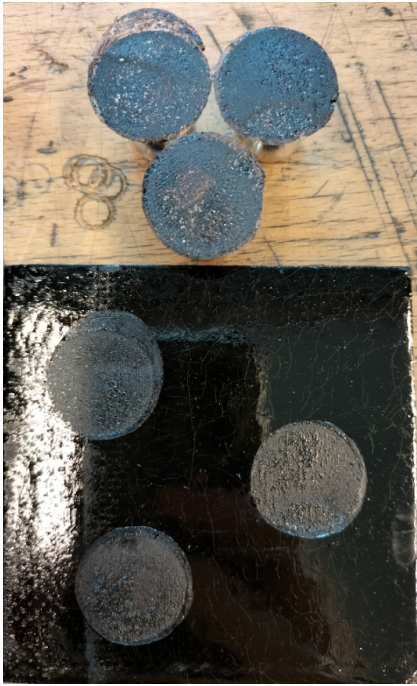


Figure 14: Typical result of a dolly pull-off test on the WTP coating, showing cohesive failure of the coating.

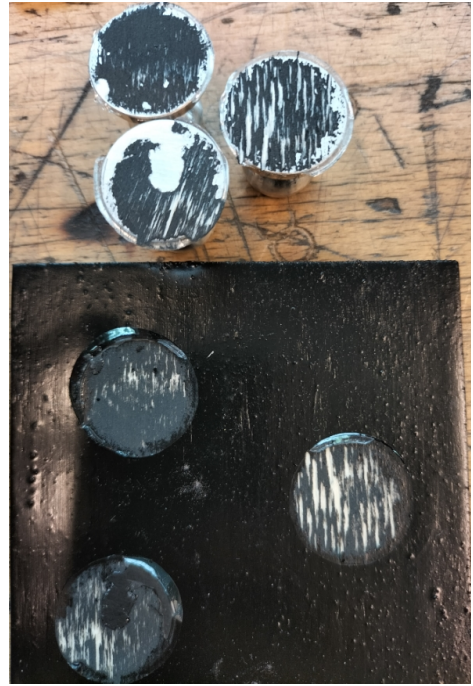


Figure 15: Typical result of the dolly pull-off on the 'Rambo' coating, showing mixed adhesive, cohesive, and substrate failure.

The 'Rambo' coating significantly increases in adhesion value after UV exposure, from 2.53 MPa to 2.95 MPa to 3.46 MPa. Although, the failure during the adhesion test also differs. Adhesion tests at t_1 were mostly failure at the glue-coating interface. While the t_2 and t_3 tests showed mixed adhesive and substrate failures. The lower 2.53 MPa value of the 'Rambo' coating is thus caused by lower glue adhesion.

4.7 Surface roughness

Confocal microscopy is used to measure the surface roughness of bare wood, the WTP coating and the 'Rambo' coating. The roughness of the WTP coating is compared to bare wood in Table 9. At 10x magnification, the only major differences are seen in R_v and K_s where the coated sample has larger values for both. The lowest valley is thus lower and the height distribution more spread out compared to bare wood.

For 50x magnification, the WTP coated sample has mostly lower values, except for the skewness. Indicating that at smaller scale, the coating is less rough than bare wood.

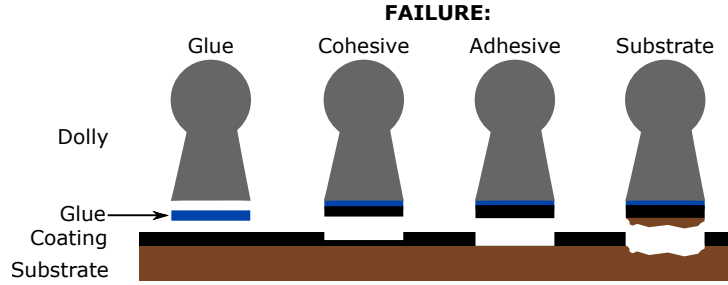


Figure 16: Illustration of different failure modes occurring during the dolly pull-off test. Left to right: glue fail (either dolly-glue or glue-coating), cohesive failure of coating, adhesive failure between coating and substrate, substrate failure.

Table 9: Roughness values comparing bare plywood to the WTP coated plywood at both 10x and 50x magnification. R_a average roughness, R_q RMS roughness, R_p highest peak, R_v lowest valley, Sk skewness, Ks kurtosis.

Sample	Magnification	R_p [μm]	R_v [μm]	R_a [μm]	R_q [μm]	Sk	Ks
WTP coated	10x	299.0	251.1	14.5	20.6	-0.09	28.58
No coat	10x	300.0	212.0	13.7	20.2	-0.08	14.10
WTP coated	50x	71.1	61.9	8.5	10.8	1.11	5.33
No coat	50x	103.1	110.1	12.4	18.3	-1.34	7.18

The roughness as function of layer thickness is plotted using the measurements done on the samples 1A-C and 2A-E from 3.3, Figure 2. As seen in Figure 17, there seems no clear relation between coating thickness and surface roughness. The thinnest layer was expected to be rougher, because it visually seemed rougher and less shiny compared to the thicker layers. As shown by the standard deviation, there can be quite a difference in R_p and R_v between measurements on the same surface. The measurement data is found in Appendix A.4 Table 12.

The surface roughness of the weathered samples is assessed by the roughness values R_a , R_q , R_p and R_v , which are plotted over weathering time in Figure 18. The measurements of both samples per timestep are averaged. For the woody thermoplastic R_p and R_v both increase within 7 days, and R_v continues to increase towards 28 days. After 28 days, R_a and R_q also increased significantly, from an initial 6 μm to 27 μm to 50 μm . The ‘Rambo’ samples show a decrease in R_p and R_v over time, while R_a and R_q stay fairly consistent at about 5 μm . The cause of the decreasing extrema is unclear. The measurement data is found in Appendix A.4 Table 13.

The effect of the UV exposure on the surface is shown in Figure 19, where the roughness values are plotted. For both coatings, an initial decrease in roughness is seen at 1 day, after which the values increase again for 3 and 7 days. This effect is stronger for the ‘Rambo’ coating.

R_a and R_q do not seem to change as much as the extrema, so overall, no clear influence of the UV light is found.

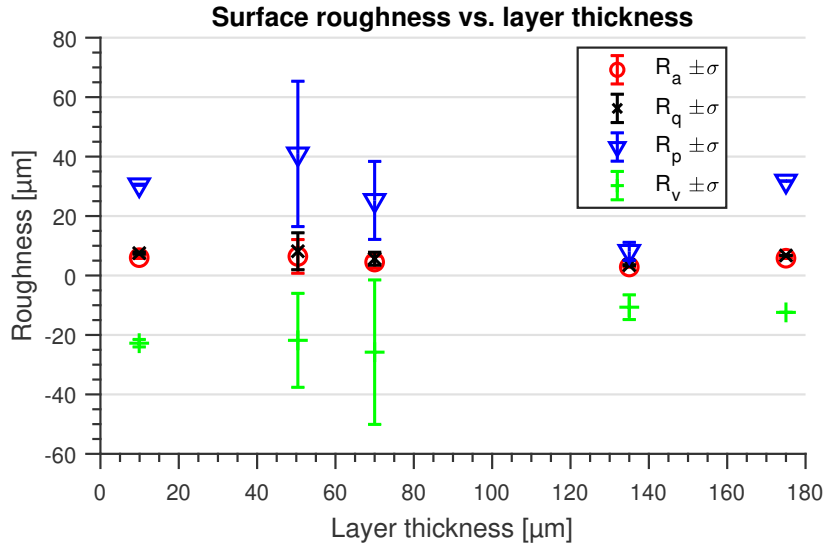


Figure 17: Surface roughness of WTP coating as function of layer thickness. Plotted are average roughness R_a , RMS roughness R_q , and the highest peak and lowest valley R_p and R_v . Mean results of two measured samples with $\pm\sigma$ errorbars, except for the thickest coat where only 1 measurement was done.

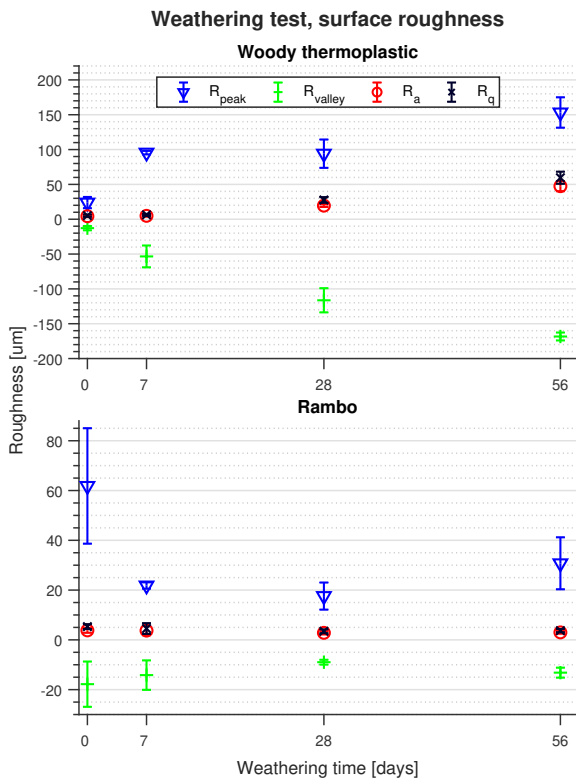


Figure 18: Natural weathering time versus surface roughness values. The average roughness R_a , the RMS roughness R_q and the peak and valley extrema R_p , R_v are shown.

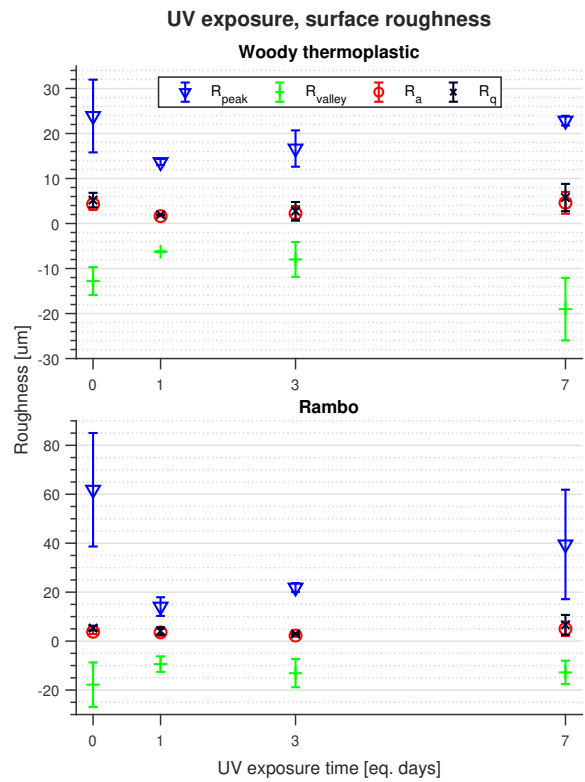


Figure 19: Surface roughness as function of UV exposure time. Plotted are the average roughness R_a , RMS roughness R_q , and the peak and valley extrema R_p and R_v . The x-axis shows the natural equivalent time of the exposure, see Table 3.

4.8 Hydrophobicity

Overall, it is found that the elliptic fit made by the ImageJ plugin is better than the circular fit, based on visual comparison of the fitted lines to the drop. In some images, the plugin failed to perform a circular fit entirely. This is also indicated by the extremely large circular standard deviation reported by the plugin, as shown in Appendix A.5.

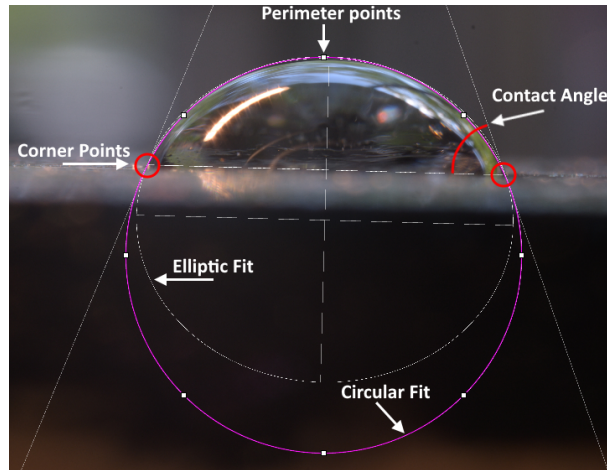


Figure 20: Output of the ImageJ contact angle plugin, showing the circular and elliptic fit. Also indicated are the ‘corner’ and perimeter points that are manually placed. The contact angle is also shown.

The contact angle on bare wood is difficult to measure, since no static drop forms on the surface. Four pictures were taken over time, resulting in a contact angle range from 41.8° to 20.0° . For the WTP coated plywood sample, 5 separate drops are measured which gives an average contact angle of 71.5° with a standard deviation of 7.5° . Thus the coating provides a good increase in hydrophobicity over bare wood. The contact angle is also measured on samples 2A-E (Figure 2), with each section an increasing layer thickness. No relation between coating thickness and contact angle is found, as shown in Table 10. The thinnest coating layer was expected to be less hydrophobic, due to the difference in visual appearance.

Table 10: Sessile drop contact angle measured on multiple coatings with varying thickness. Mean value taken over 5 separate drops.

Coating thickness [μm]	9.9	50.4	70.0	134.9	173.9
Contact angle, mean [$^\circ$]	74.3	74.4	72.2	69.8	70.6
Standard deviation, σ [$^\circ$]	2.3	3.5	4.2	4.5	4.4

The effect of natural weathering on hydrophobicity is seen in Figure 21, where the contact angle is plotted over weathering time. As already hinted at by the visual changes, ‘Rambo’ coated samples do not lose much (if any) hydrophobicity, as the contact angle stays fairly constant. The woody thermoplastic, however, quickly loses hydrophobicity within the first 7 days, a drop from 69° to 45° . After 28 days no static drop can form on the coating, thus two drops are photographed over time. Initially having a contact angle of about 72° , but quickly dropping to 36° (over the course of a few seconds).

The influence of the UV light on the contact angle is shown in Figure 22, where the contact angle is plotted against UV exposure time. Note that it is the natural equivalent time on the x-axis, not the actual exposure time (see Table 3).

As is visible, no clear relation is found between UV exposure and contact angle. The ‘Rambo’ coated samples stay fairly consistent between 85° and 90° , as to be expected from a commercial product. The WTP coated samples have a larger spread in angles, so the coating is much less consistent than the ‘Rambo’ coating, but that is not necessarily related to the UV exposure.

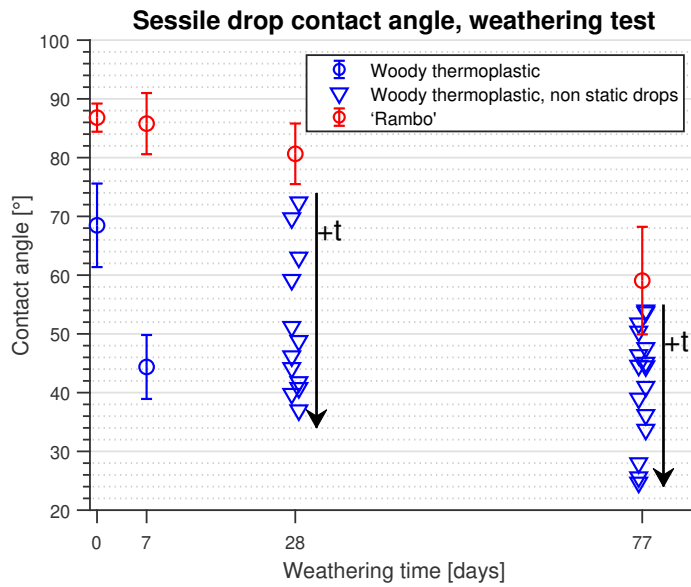


Figure 21: Contact angle of a sessile drop on both the woody thermoplastic as the Rambo coating, as function of the natural weathering time. Note that at 28 and 72 days, no static drop formed on the woody thermoplastic, thus two drops were photographed over time. Results from 5 drops averaged and standard deviation calculated.

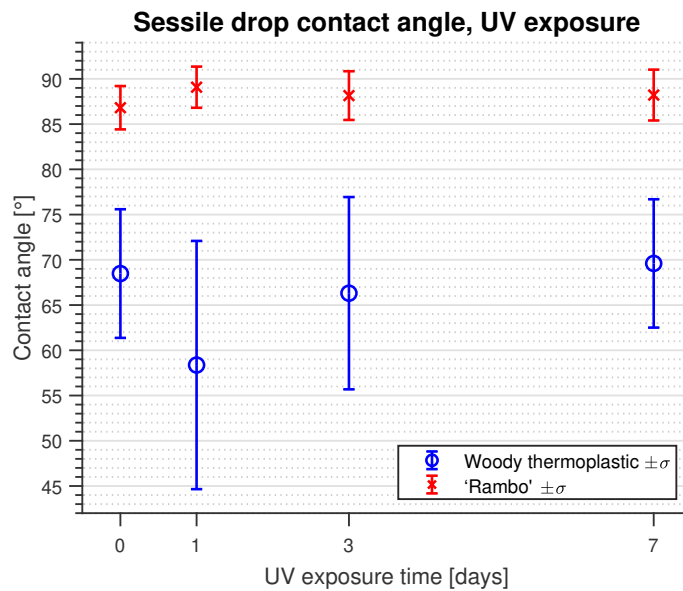


Figure 22: UV exposure time vs. the contact angle of a sessile drop on the woody thermoplastic and Rambo coating. Results from 5 drops averaged and standard deviation calculated.

5 Discussion

The rheology measurements showed common shear thinning behaviour for a thermoplastic, although the effect is more prominent for the woody thermoplastic. The melt viscosity can be compared to other plastics as seen in Figure 23 taken from Dynisco n.d., which shows a few viscosity curves of common thermoplastics at particular temperatures. Overlaid are the WTP curves from 100°C to 130°C from this report. The viscosity of the WTP is quite a bit lower than the other thermoplastics, while the temperature is also lower. Exceptions are PET and PP, but their measurement temperatures are at 285°C and 230°C. Thus in terms of processability the material is quite promising, since existing methods and processes like extrusion or injection moulding could be used. The woody thermoplastic can be processed at relatively low temperatures compared to the other examples. For example, the WTP at 100°C and 10^2 1/s has a lower viscosity than most given examples at 10^2 1/s at a significantly higher temperature. It would have been interesting to perform rheology measurements at lower temperatures, since T_g is around 50°C, there is still a decent temperature range to measure between 50-100°C.

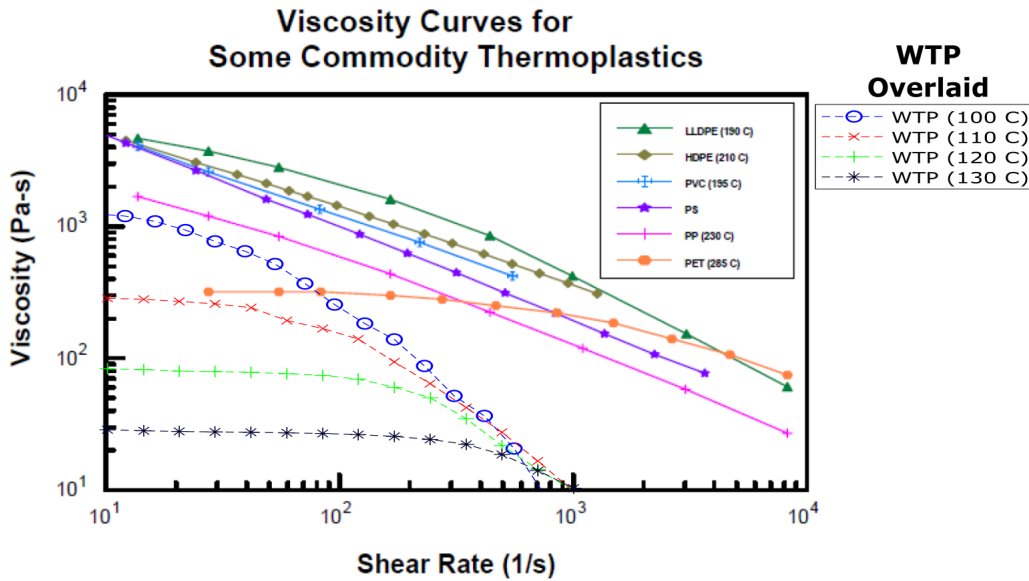


Figure 23: Viscosity curves for common thermoplastics, showing shear thinning behaviour with increasing shear rate. Taken from Dynisco n.d. Overlaid are the WTP curves from 100°C to 130 °C measured in this report.

The downside is the low glass transition temperature of the woody thermoplastic $T_g = 47^\circ\text{C}$. This is about 15°C lower than what was found by Mijnders 2018. This value can again be compared to the common thermoplastics: PP has $T_g = -15^\circ\text{C}$, PE has $T_g = -120^\circ\text{C}$, PS has $T_g = 95^\circ\text{C}$ and PVC has $T_g = 87^\circ\text{C}$. Comparable to the WTP is PA 6 and PA 11 with $T_g = 50^\circ\text{C}$ and $T_g = 45^\circ\text{C}$ respectively. So most of these materials have a T_g much higher or lower than room temperature, while the WTP and the polyamides are relatively close. However, PA 6 has a melt temperature of 223°C , which is quite high compared to the WTP, which can be considered molten about 100°C lower.

For application purpose, the glass transition may be at an awkward spot, since it is so close to room temperature that the material may go through a phase transition while in use. In a shaded environment, the temperature should thus not be warmer than about 45°C . Also taking into consideration the black colour of the material, it inherently absorbs more heat from sunlight for example. Thus in a sunny environment, the environment temperature is even more limited.

Based on the rheology data and T_g , the material may be applicable indoors, or shaded areas outdoors that do not reach hotter temperatures. Application above T_g does not seem ideal, due to the low viscosity found at 100°C .

Regarding the solvent painting, the main issue arose in determining the coating thickness. The initial approach of measuring coated and uncoated locations was obviously not great, the second attempt (mea-

suring before and after coating) was better, but still relied on manual placement and measurements. The coating thickness may therefore not be entirely accurate. The main goal was to get an idea of the thickness, and since no further measurements rely on the coating thickness, it is sufficient for now.

The tape pull tests provided a promising result to pursue the dolly testing. The tape pulls could have been done more consistently, since on the 3rd and 4th test the tape was pushed down harder around the cuts. The difference in method is not too significant and the results are easily explained. The tape of the 3rd and 4th test simply show darker lines at the cut locations, since more material is pulled off.

The dolly pull-off results are trickier to assess, since the failure modes are somewhat complex. The results depend on the cohesion of the substrate and the coating, and also depends on the adhesion of the substrate-coating, the coating-glue, and the glue-dolly interface. For the WTP, most failure is cohesive due to the weak material. This does indicate that the actual adhesion is larger than the found value. When the failure is mixed, purely comparing values is not an option, which is why the failure types were classified. But even then, the ratio in mixed failures may be different, leading to different adhesion values.

The setup used for the contact angle measurements is somewhat improvised with readily available materials, but the principle is similar to scientific equipment. In the used setup, the drop size is not consistent, and the camera angle is slightly different between measuring sessions. The accuracy might therefore not be as good, but the results are clear, so the accuracy is likely not an issue.

For comparison, Diversified Enterprises n.d., gives an overview of contact angles of water on various polymers. Comparable to the woody thermoplastic is Nylon 12 (72.4°) and PET (72.5°). The smallest contact angles given are for polyvinyl alcohol (PVOH) at 51°, and polyvinyl acetate (PVAc) with 60.6°. The largest angle is 112° of butyl rubber (polyisobutylene). Thus, the woody thermoplastic is no outlier in terms of contact angle when compared to other polymers, but it does sit more at the lower end of the spectrum.

A proper weathering test should be 12 full months, such that all seasons and weather conditions come by. Since the test only lasted a few months, the result is thus an intermediate result. This is not much of an issue, since the WTP coating degraded quickly and the results are clear. Still, it would be interesting to see if the degradation occurs in the same manner during colder days, potentially with less direct sun. During the weathering experiment, it becomes clear that the woody thermoplastic degrades rather quickly. It is not uncommon for polymers to degrade outdoors, but understanding what causes the degradation in the woody thermoplastic may give ideas on how to prevent it.

On a chemical level, the degradation of the polymer may be explained based on the structure of the polymer. Physical ageing of a polymer can be caused by UV in combination with oxygen (photo-oxidation), but also other reactions like ozonolysis (mainly for rubbers) and hydrolysis. The main influence is suspected to be photo-oxidation. Photo-oxidation occurs when a photon is absorbed by chromophores in the material. Absorption may either be inherent to the polymer or absorbing impurities may be present. The absorption can break some bonds, which creates free radicals, which in turn may cause further degradation reactions (Wiles and Carlsson 1980). Feldman 2002 states that saturated compounds with C-C, C-H, O-H, and C-Cl absorb wavelengths shorter than 200 nm, while carbonyl groups and conjugated double bonds mostly absorb in the 200-300 nm range. Rao et al. 2022 states that wavelengths of 346 nm, 334 nm, and 289 nm are required to break C-C, C-O, and C-H bonds respectively.

Focusing more on biomass, lignin is pointed out as the sensitive component when it comes to photo-oxidation. It is found that bamboo absorbed about 80% of UV light, with peak absorption occurring at 280 nm. The Norrish Type-I reaction in Figure 24 is one of the reactions that occur in the degradation. (Rao et al. 2022)

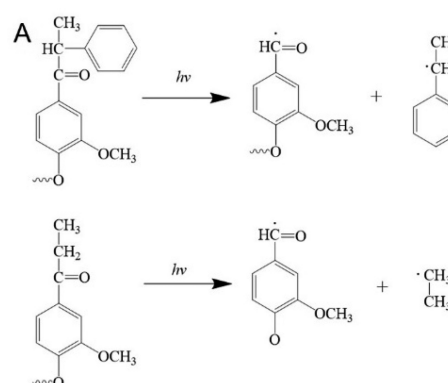


Figure 24: Norrish type-I photo-oxidation reaction of lignin. From Rao et al. 2022

6 Conclusion and recommendations

The goal of the thesis is to find out if a biomass based thermoplastic can be a useful material for a wood coating. As stated in the objectives, the first question is to figure out: ‘what makes a good coating material?’. Based on literature and test standards, the adhesion of the coating, its resistance to weathering, and the hydrophobicity are selected as important test parameters for a coating. The importance of adhesion may be obvious: if the coating does not adhere, then all other properties are irrelevant, since the material does not stay on the substrate to do its job. The application of the woody thermoplastic may be outdoors, hence the weathering resistance is found important. Related is the hydrophobicity, since wood is quite sensitive to moisture. If the coating can therefore repel water drops, it may provide protection against rain and moisture.

Next to these investigated properties one may for example also consider impact resistance, or visual appearance, depending on the application.

As became clear during the tests and measurements, the woody thermoplastic can be used as a coating, but it is not ideal. The adhesion is limited by the material strength, which is rather low currently, but this does mean that there is improvement to be made. The main issue is the degradation due to weathering, as the coating degraded within weeks. The hydrophobicity is good enough, albeit on the lower end for polymers. Unfortunately, it also quickly degrades due to the weathering. So overall, the material may be usable as a coating, but it does still need improvement. As was also discussed in the previous section.

While the first two objectives focused more on investigating the material itself, the third objective is to find suitable production methods. Based on the thermal properties of the woody thermoplastic, extrusion is a straightforward method used for many thermoplastics. The glass transition temperature and the melt range for the woody thermoplastic are relatively low, and shear thinning behaviour is observed, making extrusion a good option. And as was found in literature (Järvelä et al. 1999; Kuusipalo 2001), extrusion of thermoplastics can be used to produce coatings on wood.

As is done in this thesis, the woody thermoplastic can be made into paint, which is a simple method that can be used on multiple scales. Consumers can use it at home by brushing or rolling, while spray painting may be considered for larger scale, and industrial applications.

Powder coating may also be considered, although it is slightly more involved setup. Powder coating is normally used on metal substrates, but it is supposedly possible to do on wood. It is currently not known if the woody thermoplastic material is suitable for powder coating, since the powder coating gun needs to be able to charge the material particles.

One final method that was considered is 3D printing, which in some way is similar to extrusion. A relatively simple setup was found in the form of a 3D printer for chocolate (MarVtec 2019). A heating element is wrapped around a large syringe, which is actuated by a motor to extrude the molten material from the syringe. The syringe is attached to a common 3D printer XYZ stage.

Recommendations

It is clear now that work on this material is far from done, recommendations for future work are therefore needed.

As is already found in the previous work, the material is quite brittle and not very strong. Supposedly, the adhesion values are therefore also not as good as they can be. Increasing the material strength and reducing brittleness may thus be needed. An obvious improvement is increasing the molecular weight, since the molecular weight is linked to physical properties of the material. For example, a higher weight average molecular weight (\overline{M}_w) increases the glass transition temperature. Since the current T_g is quite low, this may be a welcome change. \overline{M}_w also affects the viscosity, which is relatively low compared to other thermoplastics, so an increase there should also not be an immediate issue. To reduce brittle failure, a higher molar mass should help as well. Particularly the number average molar mass \overline{M}_n is important for brittle failure (Vegt 2006). Since $\overline{M}_n = \sum n_i \cdot M_i$, either the amount of chains (n_i) needs to increase or the chains need to become heavier (increase M_i). Achieving a higher molecular weight might not be so easy, however. The effect of multiple liquefaction runs and different source material on molecular weight was already shown in Ruiz et al. 2019. Thus it is not expected that more liquefaction runs or a different source material will bring significant improvements.

Also investigated earlier is the addition of short bagasse fibres to the WTP, which increases the tensile

strength to 2.5 MPa. Perhaps using the short fibre blend as coating material produces a more durable coating.

Photo-oxidation due to UV exposure would still be an issue that needs to be fixed. The first step is to figure out which wavelengths are absorbed by the material, such that an appropriate solution can be found. This can be done with a spectrophotometer, which will measure the wavelengths that either reflect from, or pass through the sample material. The absorbed wavelengths will then also be known. It is expected that the material absorbs wavelengths in the 300-400 nm range. Since the interest is in the UV wavelength, the device should of course be able to measure UV wavelengths. It will then be clear which wavelengths are absorbed, and which wavelengths may therefore be a problem with regards to ageing.

Additives are available for the purpose of photo-stabilisation or anti-oxidation, but choosing the right one is a task in itself. The additive should of course fit in the sustainable picture of the woody thermoplastic, and it should provide enough protection without unwanted side-effects. The additive should also be suitable to be processed and recycled. As mentioned by Feldman 2002, UV absorbers need a certain depth to absorb properly, the use on polymer surfaces and thin items is thus not ideal. Currently, carbon black and TiO_2 are commonly used. Wiles and Carlsson 1980 suggest, that for UV stabilisation of PP, PVC, PC (and others) about 0.1-1% wt. of additives can be used. As suggested by Rao et al. 2022, applying a transparent, UV stabilising coating on top of the WTP coating may protect it from UV light and thus degradation. The difficulty of an extra coating is the recyclability of the end product.

The use of acetone as a solvent to make the paint also may not fit in the sustainable approach of the project. For small scale testing, the use of acetone is the easiest option as it is readily available, but a better alternative should be investigated. A short literature search does however not point to any major issues with acetone, but it should be investigated further. Biomass based acetone (bio-acetone) is available and may be a good option.

If solvents need to be avoided altogether, other production methods like extrusion may be considered as already mentioned earlier.

The artificial weathering performed so far can be expanded further. Next to UV exposure, there were plans to expose the coating to heat in an oven, which is now left as a recommendation. Additionally, the coating could be exposed to moisture by controlling the air humidity, or by forcing steam onto the coating.

References

- Bisinella, Valentina, Paola Federica Albizzati, et al. (Feb. 2018). *Life Cycle Assessment of grocery carrier bags*. Tech. rep. The Danish Environmental Protection Agency. URL: <https://www2.mst.dk/Udgiv/publications/2018/02/978-87-93614-73-4.pdf>.
- Brugnara, Marco (2006). *Contact Angle*. <https://imagej.nih.gov/ij/plugins/contact-angle.html>. ImageJ Plugin, last accessed on 07-05-2022.
- CAMAG (2016). *Instruction manual UV lamp 4, UV cabinet 4*. <https://chemoquip.co.za/docs/pharmaceutical/UV%20Cabinet%20&%20Lamp.pdf>. last accessed on 17-07-2022.
- Diversified Enterprises (n.d.). *Critical Surface Tension and Contact Angle with Water for Various Polymers*. https://www.accudynetest.com/polytable_03.html?sortby=contact_angle. last accessed on 13-05-2022.
- Dynisco (n.d.). *Practical Rheology Section 3*. last accessed on 12-09-2022. URL: https://www.dynisco.com/userfiles/files/Practical_Rheology_Section_3.pdf.
- Feldman, D. (2002). “Polymer Weathering: Photo-Oxidation”. In: *Journal of Polymers and the Environment* 10 (4), pp. 163–173. ISSN: 1572-8900. DOI: <https://doi.org/10.1023/A:1021148205366>.
- Geyer, Roland, Jenna R. Jambeck, et al. (2017). “Production, use, and fate of all plastics ever made”. In: *Science Advances* 3.7, e1700782. DOI: <https://doi.org/10.1126/sciadv.1700782>. URL: <https://www.science.org/doi/abs/10.1126/sciadv.1700782>.
- Gradus, Raymond H.J.M., Paul H.L. Nillesen, et al. (2017). “A Cost-effectiveness Analysis for Incineration or Recycling of Dutch Household Plastic Waste”. In: *Ecological Economics* 135, pp. 22–28. ISSN: 0921-8009. DOI: <https://doi.org/10.1016/j.ecolecon.2016.12.021>.
- Hazir, Ender and Küçük Huseyin Koc (Dec. 2019). “Evaluation of wood surface coating performance using water based, solvent based and powder coating”. In: *Maderas. Ciencia y tecnología* 21, pp. 467–480. ISSN: 0718-221X. DOI: <https://doi.org/10.4067/S0718-221X2019005000404>.
- Järvelä, P.K., O. Tervala, et al. (1999). “Coating plywood with a thermoplastic”. In: *International Journal of Adhesion and Adhesives* 19.4, pp. 295–301. DOI: [https://doi.org/10.1016/S0143-7496\(98\)00075-X](https://doi.org/10.1016/S0143-7496(98)00075-X).
- Kajaks, J. A., G. G. Bakradze, et al. (2009). “The use of polyolefins-based hot melts for wood bonding”. In: *Mechanics of Composite Materials* 45.6, pp. 643–650. DOI: <https://doi.org/10.1007/s11029-010-9120-7>.
- Kuusipalo, J. (2001). “Plastic Coating of Plywood Using Extrusion Technique”. In: *Silva Fennica* 35.1, pp. 103–110. DOI: <https://doi.org/10.14214/sf.607>.
- MarVtec (2019). *Chocolate 3D printer, chocolate extruder*. last accessed on 01-10-2022. URL: <https://www.thingiverse.com/thing:3511736>.
- Mijnders, J. (2018). “Reinforced Vacuum Residue From Biomass Liquefaction oil as a thermoplastic”. MSc Thesis, Sustainable Process Technology.
- National Renewable Energy Laboratory (n.d.). *Reference Air Mass 1.5 Spectra*. <https://www.nrel.gov/grid/solar-resource/spectra-am1.5.html>. last accessed on 16-07-2022.
- Nogova, B. (2019). “Improving Mechanical Properties Of Woody Thermoplastic”. MSc Thesis, Sustainable Process Technology.
- Norvydas, Valdas and Darius Minelga (2006). “Strength and Stiffness Properties of Furniture Panels Covered with Different Coatings”. In: *Materials Science (MEDŽIAGOTYRA)* 12.4, pp. 328–332. URL: <https://matsc.ktu.lt/index.php/MatSc/article/view/26469>.
- Oliveux, Géraldine, Luke O. Dandy, et al. (2015). “Current status of recycling of fibre reinforced polymers: Review of technologies, reuse and resulting properties”. In: *Progress in Materials Science* 72, pp. 61–99. ISSN: 0079-6425. DOI: <https://doi.org/10.1016/j.pmatsci.2015.01.004>. URL: <https://www.sciencedirect.com/science/article/pii/S0079642515000316>.
- Padmanabhan, Sambandam, K. Giridharan, et al. (Mar. 2022). “Energy recovery of waste plastics into diesel fuel with ethanol and ethoxy ethyl acetate additives on circular economy strategy”. In: *Scientific Reports* 12 (1), p. 5330. DOI: <https://doi.org/10.1038/s41598-022-09148-2>.
- Pimenta, Soraia and Silvestre T. Pinho (2011). “Recycling carbon fibre reinforced polymers for structural applications: Technology review and market outlook”. In: *Waste Management* 31.2,

- pp. 378–392. ISSN: 0956-053X. DOI: <https://doi.org/10.1016/j.wasman.2010.09.019>. URL: <https://www.sciencedirect.com/science/article/pii/S0956053X10004976>.
- Rao, Fei, Xiaoyan Li, et al. (2022). “Photodegradation and Photostability of Bamboo: Recent Advances”. In: *ACS Omega*. DOI: <https://doi.org/10.1021/acsomega.2c02035>.
- Ritchie, H. (Oct. 2018). *FAQ on plastics*. <https://ourworldindata.org/faq-on-plastics#are-plastic-alternatives-better-for-the-environment>. Last accessed on: 15-07-2022.
- Ruiz, M. Pilar, Janine Mijnders, et al. (2019). “Fully Recyclable Bio-Based Thermoplastic Materials from Liquefied Wood”. In: *ChemSusChem* 12.19, pp. 4395–4399. DOI: <https://doi.org/10.1002/cssc.201901959>.
- Tournier, V., C. M. Topham, et al. (Apr. 2020). “An engineered PET depolymerase to break down and recycle plastic bottles”. In: *Nature* 580 (7802), pp. 216–219. DOI: <https://doi.org/10.1038/s41586-020-2149-4>.
- Vegt, A.K. van der (2006). *From polymers to plastics*. Delft, The Netherlands: VSSD. URL: <https://delftacademicpress.nl/m028.php>.
- Wiles, D.M. and D.J. Carlsson (1980). “Photostabilisation mechanisms in polymers: A review”. In: *Polymer Degradation and Stability* 3 (1), pp. 61–72. ISSN: 0141-3910. DOI: 10.1016/0141-3910(80)90008-7.
- Zheng, Jiajia and Sangwon Suh (May 2019). “Strategies to reduce the global carbon footprint of plastics”. In: *Nature Climate Change* 9 (5), pp. 374–378. DOI: <https://doi.org/10.1038/s41558-019-0459-z>.

A Appendix

A.1 Rheology, amplitude sweep

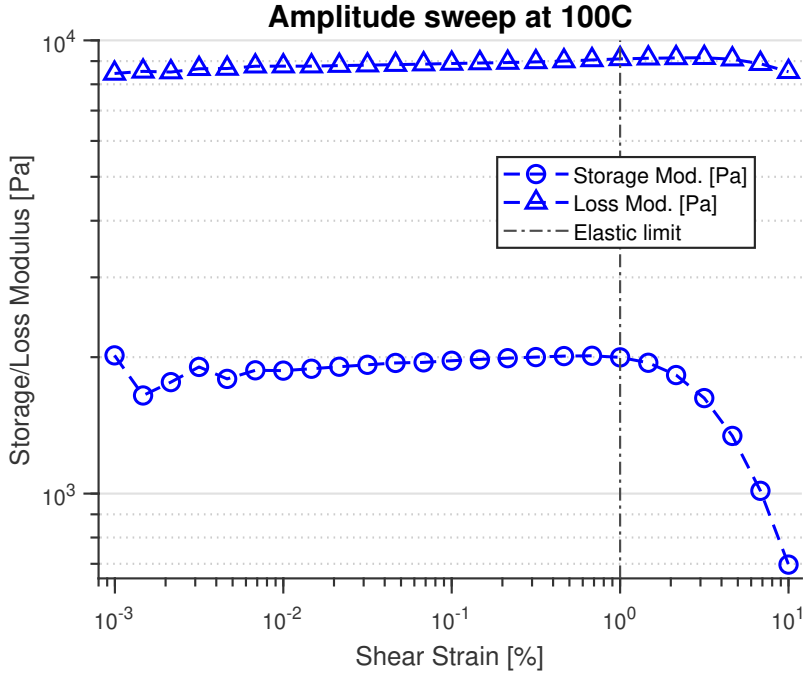


Figure 25: Amplitude sweep performed at 100°C with a plate-plate geometry. Plotted is the storage and loss modulus as function of shear strain. The elastic limit is determined to be at 1% strain.

A.2 Rheology, storage and loss modulus

Separate plots of the storage and loss modulus at each temperature are shown in Figure 28. From this data, a master curve can be created by using time-temperature superposition. The master curve spans a larger range of frequencies than a single measurement can provide, thus resulting in data beyond the practical measurement range. The curves shown in Figure 26 are composed of the individual measurements which are horizontally shifted by a factor a_T , for the loss and storage measurements this means that the frequencies are $\omega_{shift} = a_T \cdot \omega_{measured}$. A master curve for the complex viscosity is also made, as shown in Figure 27. The complex viscosity is calculated with

$$|\eta^*| = \frac{\sqrt{G'{}^2 + G''{}^2}}{\omega}$$

. The shift factor is determined by trial and error, until the shifted data visually aligns with the ‘reference’ temperature.

For the performed measurements, 130°C is chosen as the reference, thus all other measurements are shifted to align with the data at 130°C. This provides data-points both above and below the frequencies measured. The determined shift factors are shown in Table 11.

Table 11: Horizontal shift factors used with time-temperature superposition. $a_T > 1$ is a shift to the right, $a_T < 1$ is a shift to the left.

Temperature (°C)	100	110	120	130	140	150	160
Shift factor a_T	76.4	19.5	4.0	1.0	0.3	0.2	0.11

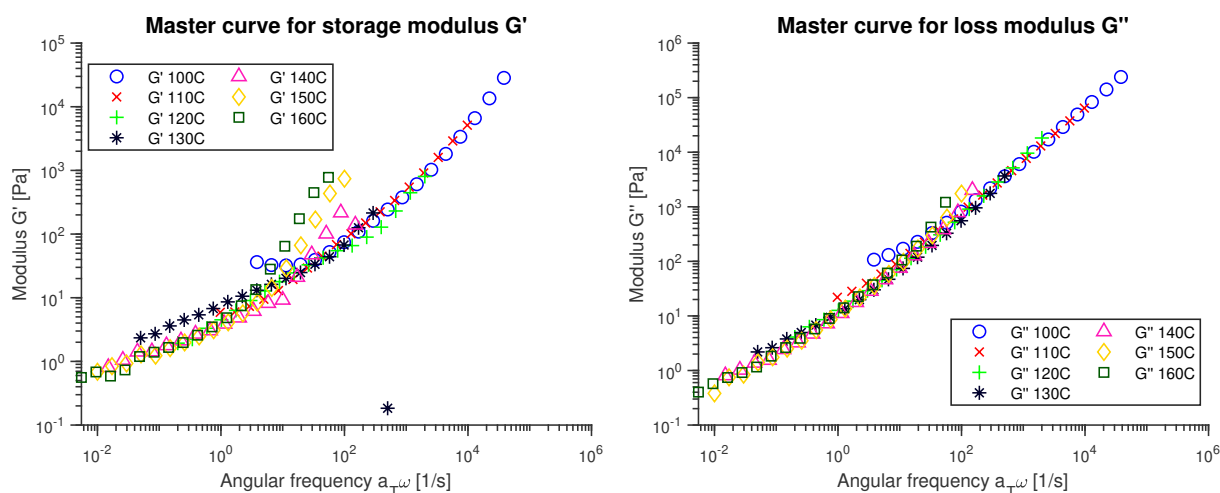


Figure 26: Master curves of storage modulus (left) and loss modulus (right) with a reference temperature of 130°C. Plotted as function of angular frequency. Shift factors are listed in Table 11.

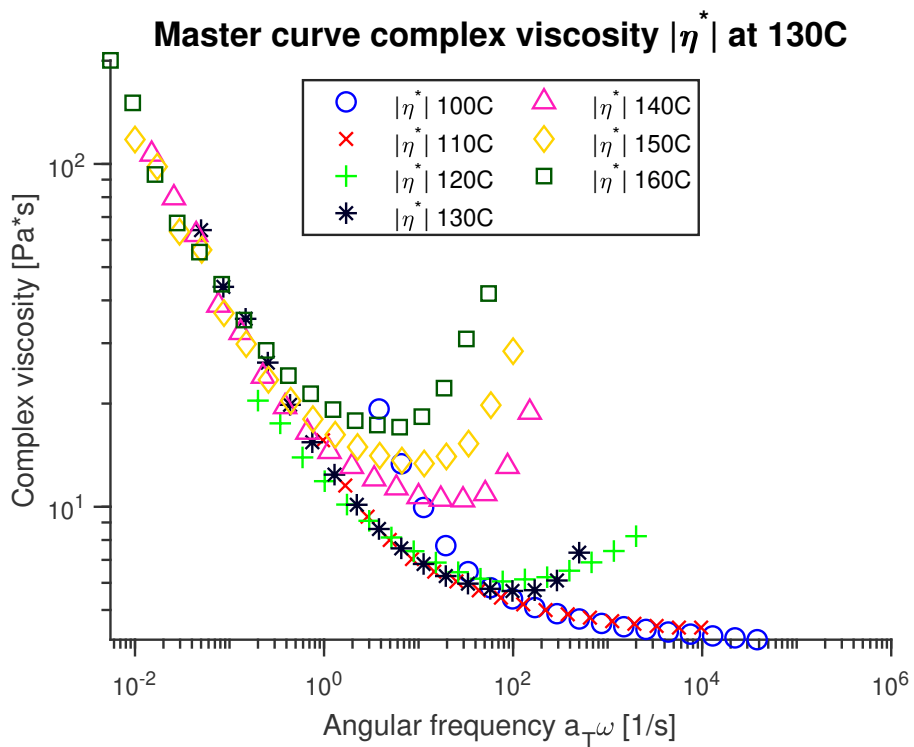


Figure 27: Master curve for the complex viscosity as function of angular frequency. Shifted to a reference temperature of 130°C.

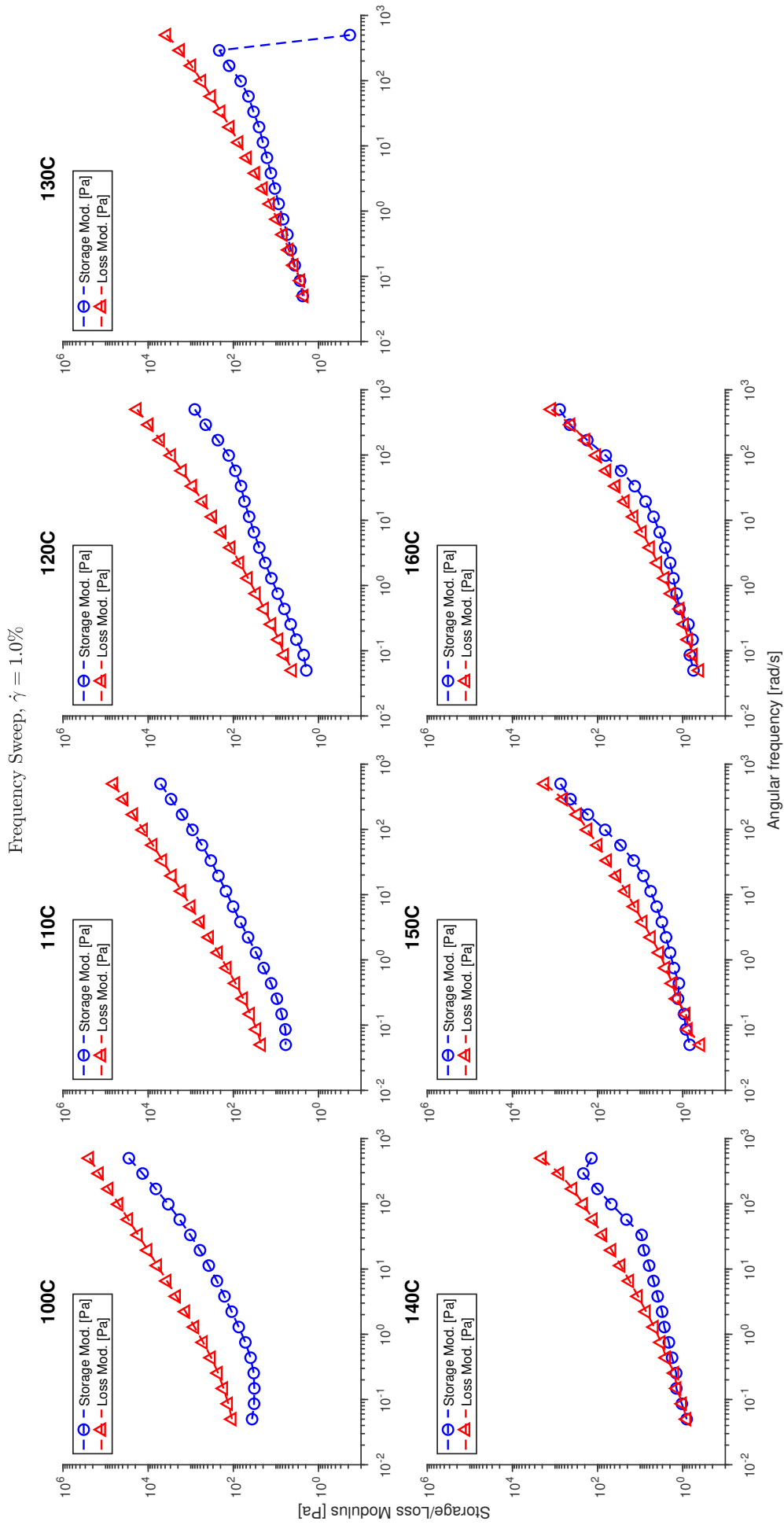


Figure 28: Rheology frequency sweeps for temperatures of 100°C to 160°C. For each temperature the loss and storage modulus are plotted a function of the angular frequency.

A.3 Submersed samples



Figure 29: Picture of the submersed samples taken after 14 days. Left to right: woody theroplastic, ‘Rambo’, and bare wood.

A.4 Roughness data

Table 12: Roughness data for various samples: No. 1 and 2 sections A-E: woody thermoplastic (WTP) coating (with increasing thickness) on solid pine wood.

With R_p the highest peak, R_v the lowest valley, R_a average roughness, R_q RMS roughness, Sk the Skewness and Ks the Kurtosis.

Sample	Coat thickness [μm]	Magn.	R_p [μm]	R_v [μm]	R_a [μm]	R_q [μm]	Sk	Ks
1A	9.9	50x	30.385	21.884	5.823	7.263	0.1313	3.3564
2A	$\approx 10^1$	50x	30.654	23.663	6.192	7.787	0.2802	2.9879
1B1	50.4	50x	15.523	7.695	2.326	3.070	0.6847	3.9673
1B2	50.4	50x	42.892	38.887	12.892	15.078	-0.3473	1.9441
2B	$\approx 50^1$	50x	64.297	18.854	4.042	6.331	2.8826	19.6610
1C	70.0	50x	15.983	8.607	3.096	4.102	0.7948	3.5303
2C	$\approx 70^1$	50x	34.542	42.974	5.943	7.189	0.2310	2.4456
2D1	$\approx 135^1$	50x	5.987	13.602	2.898	3.596	-0.9364	3.5318
2D2	$\approx 135^1$	50x	10.267	7.724	2.820	3.380	-0.1374	2.3542
2E	$\approx 175^1$	50x	31.769	12.409	5.811	6.736	0.1802	1.8966

¹ Thickness of sample 2 sections A-E are not measured, but estimated to be similar to the thickness of sample 1 section A-E.

Table 13: Overview of roughness data of the weathering experiment. Measured at 50x magnification using a Keyence VK confocal microscope. Woody thermoplastic (WTP), ‘Rambo’ (RM) reference paint. R_p highest peak, R_v lowest valley, R_a average roughness, R_q RMS roughness, Sk Skewness, Ks Kurtosis.

Sample	Weather time [days]	Magn.	R_p [μm]	R_v [μm]	R_a [μm]	R_q [μm]	Sk	Ks
WTP Pre1	0	50x	31.966	9.707	3.039	3.598	-0.3527	2.8166
WTP Pre2	0	50x	15.796	15.889	5.546	6.824	0.1567	2.3751
WTP t1-1	7	50x	98.160	37.713	6.074	7.729	0.1355	3.2634
WTP t1-2	7	50x	93.016	69.092	3.663	4.846	-1.3460	25.0166
WTP t2-1	28	50x	73.774	99.036	17.659	23.568	-1.0604	4.7074
WTP t2-2	28	50x	114.436	133.727	21.330	31.704	-1.7930	7.7787
WTP t3-1	77	50x	175.008	174.029	40.262	50.892	0.1846	3.9336
WTP t3-2	77	50x	131.424	162.664	54.594	68.273	-0.7410	2.6198
RM Pre1	0	50x	38.650	26.895	4.758	6.267	1.4227	6.8076
RM Pre2	0	50x	85.030	8.705	2.851	4.347	5.9264	75.7142
RM t1-1	7	50x	20.565	8.250	1.896	2.400	-0.1335	4.1645
RM t1-2	7	50x	23.108	20.078	5.537	6.702	-0.2092	2.5888
RM t2-1	28	50x	12.151	7.998	2.169	2.685	-0.4471	2.2475
RM t2-2	28	50x	23.034	9.938	3.481	4.218	0.0043	2.2643
RM t3-1	77	50x	20.313	11.171	2.489	3.035	-0.4052	2.6582
RM t3-2	77	50x	41.197	15.174	3.506	4.358	0.0327	3.3027

Table 14: Roughness data averaged over 2 measurements with their standard deviation. Average roughness R_a , RMS roughness R_q , and the peak and valley extrema R_p and R_v . All values in [μm]

Samples	Exposure [days]	R_p	σ_{Rp}	R_v	σ_{Rv}	R_a	σ_{Ra}	R_q	σ_{Rq}
WTP pre	0	23.88	8.09	12.80	3.10	4.29	1.25	5.21	1.61
WTP t1	1	13.65	0.68	6.27	0.11	1.63	0.03	1.97	0.01
WTP t2	3	16.66	4.03	7.98	3.86	2.25	1.65	2.75	2.02
WTP t3	7	22.86	1.08	19.02	6.95	4.61	2.43	5.77	3.04
RM pre	0	61.84	23.19	17.80	9.10	3.80	0.95	5.31	0.96
RM t1	1	14.10	3.81	9.40	3.15	3.54	1.40	4.10	1.51
RM t2	3	21.87	1.80	13.12	5.74	2.28	0.46	2.95	0.42
RM t3	7	39.50	22.37	12.79	4.80	5.01	2.92	6.64	4.05

A.5 Contact Angle data

Table 15: Table of all relevant data gathered from the ImageJ Contact Angle plugin. With θ the determined contact angle. The plugin makes a circular and elliptic fit and outputs the standard deviation of both fits. Note that the ellipse is a better fit.

Sample T1 WTP coated plywood, R1 bare wood, 2A-E coated pine wood with increasing layer thickness.

Sample	θ Circle	θ Left	θ Right	θ Ellipse	Circle St.Dev.	Ellipse St.Dev.
T1	61.5	65.4	64.5	65.0	1.52	2.14e-03
T1	68.0	76.6	77.6	77.1	4.10	1.66e-03
T1	67.1	74.4	74.1	74.2	3.42	2.29e-03
T1	55.4	63.6	60.7	62.2	2.74	1.60e-03
T1	64.8	81.6	76.6	79.1	6.25	1.29e-03
R1	122.1	42.8	40.7	41.8	7.23e+08	2.50e-03
R1	17.9	20.8	23.8	22.3	2.28	5.93e-03
R1	117.8	30.0	34.9	32.4	6.77e+08	7.22e-03
R1	92.0	16.4	23.6	20.0	1.35e+09	3.24e-03
2A	68.5	75.4	74.1	74.8	2.98	3.48e-03
2A	71.3	77.1	76.4	76.8	2.24	2.85e-03
2A	66.5	74.9	76.7	75.8	4.21	2.09e-03
2A	61.6	70.2	74.6	72.4	6.12	1.03e-03
2A	65.6	70.8	72.0	71.4	2.53	3.39e-03
2B	66.2	80.6	77.3	79.0	6.49	1.09e-03
2B	57.5	73.0	68.9	71.0	6.44	9.18e-04
2B	68.1	78.4	72.5	75.4	4.07	1.91e-03
2B	61.4	70.7	70.7	70.7	4.96	2.29e-03
2B	68.2	76.9	74.6	75.8	3.64	1.09e-03
2C	68.5	81.0	77.6	79.3	5.04	1.26e-03
2C	65.3	70.8	71.5	71.2	1.96	2.11e-03
2C	60.7	68.6	69.6	69.1	4.39	2.33e-03
2C	57.3	70.0	67.8	68.9	4.39	1.30e-03
2C	61.7	73.3	71.5	72.4	4.91	2.26e-03
2D	70.3	77.1	77.0	77.1	3.17	3.34e-03
2D	63.2	71.8	69.0	70.4	3.56	1.84e-03
2D	58.0	67.3	66.1	66.7	4.63	2.35e-03
2D	61.4	67.3	63.7	65.5	2.26	2.01e-03
2D	57.2	71.9	67.0	69.4	6.79	1.36e-03
2E	69.6	74.5	74.4	74.4	2.10	2.87e-03
2E	59.0	66.5	66.2	66.4	3.75	3.34e-03
2E	65.2	72.0	71.6	71.8	3.41	1.21e-03
2E	63.4	76.6	73.4	75.0	6.02	1.35e-03
2E	57.9	67.0	64.4	65.7	4.07	3.05e-03

PAPER NAME

23-10-22 MSc Project Report - Final Draft(1).pdf

AUTHOR

-

WORD COUNT

16297 Words

CHARACTER COUNT

77775 Characters

PAGE COUNT

36 Pages

FILE SIZE

13.0MB

SUBMISSION DATE

Oct 25, 2022 10:22 AM GMT+2

REPORT DATE

Oct 25, 2022 10:25 AM GMT+2

● 2% Overall Similarity

The combined total of all matches, including overlapping sources, for each database.

- 2% Internet database
- 1% Publications database
- Crossref database
- Crossref Posted Content database
- 0% Submitted Works database

● Excluded from Similarity Report

- Bibliographic material
- Quoted material
- Small Matches (Less than 8 words)